TAMPEREEN TEKNILLINEN YLIOPISTO
TAMPERE UNIVERSITY OF TECHNOLOGY

JAN VILJANEN

MICROWAVE ENHANCED LASER INDUCED BREAKDOWN SPECTROSCOPY AT ATMOSPHERIC PRESSURE

Master of Science thesis

Examiner: Dr. Juha Toivonen
Examiner and topic approved by the
Faculty Council of the Faculty of
Natural Sciences
on 3rd June 2015

ABSTRACT

JAN VILJANEN: Microwave Enhanced Laser Induced Breakdown Spectroscopy at Atmospheric Pressure
Tampere University of Technology
Master of Science thesis, 50 pages
July 2015
Master's Degree Programme in Science and Engineering
Major: Applied Physics
Examiner: Dr. Juha Toivonen
Keywords: LIBS, microwave, plasma, antenna

Laser induced breakdown spectroscopy (LIBS) has become one of the most intriguing optical spectroscopical elemental analysis methods. It exhibits great features, such as simplicity, information richness, stand-off ability and practically no sample preparation requirements. Even though there has been, and is, a vast interest and effort toward developing the technique to become the standard in every laboratory, the main drawbacks are yet to overcome. LIBS falls behind its rivals, i.e., inductively-coupled plasma spectroscopy and chemical analysis, in quantitative analysis and in sensitivity. Different methods has been developed to enhance LIBS measurement; double pulse LIBS, spatial confinement and microwave enhancement.

In this thesis, the sensitivity of LIBS measurement in atmospheric pressure is improved by applying antenna-coupled microwave radiation to the plasma plume induced by pulsed laser radiation on solid sample. Applied microwave radiation reheats the plasma and prolongs the plasma lifetime. This enables use of longer signal integration times and therefore signal intensities are improved.

LIBS signal enhancement by antenna-coupled microwave radiation on solid samples at atmospheric pressure was introduced for the first time in performed measurements. For detection limit, an enhancement factor of 93 was achieved for low energy laser pulse. The detection limit of copper was improved down to 8.1 ppm. As antenna-coupled microwave enhancement is relatively simple and inexpensive enhancement method, it shows excellent potential to be developed further in to a versatile application for needs of different fields of industry and science. With careful antenna design and by optimizing the antenna positioning the method can be further improved.

TIIVISTELMÄ

JAN VILJANEN: Mikroaaltoavustettu laser-indusoitu hajoitusspektroskopia normaalissa ilmanpaineessa
Tampereen teknillinen yliopisto
Diplomityö, 50 sivua
Heinäkuu 2015
Teknis-luonnontieteellinen koulutusohjelma
Pääaine: Teknillinen fysiikka
Tarkastaja: Dr. Juha Toivonen
Avainsanat: LIBS, mikroaalto, plasma, antenni

Laser indusidusta hajoitusspektroskopiasta (LIBS) on tullut viime vuosikymmenen aikana yksi tutkituimmista ja suosituimmista optisen alkuainespektroskopian menetelmistä. LIBS:n suosion salaisuus on sen yksinkertaisuudessa ja erityisesti siinä, ettei mitattavat näytteet vaadi juurikaan valmisteluja. Syyt, miksi LIBS laitteisto ei ole noussut jokaisen kemian laboratorion pöydälle, ovat sen hankaluudet kvantitatiivisessa mittauksessa ja heikossa herkkyydessä kilpailijoihin verrattuna. LIBS:n heikkouksiin on pyritty luomaan ratkaisua erilaisilla menetelmillä, kuten kaksoispulssi LIBS, plasman tiivistäminen ja mikroaaltoavustus.

Tämän diploityön tavoitteena on parantaa kinteästä näytteestä saatavan LIBS signaalin herkkyyttä käyttäen anteenniin kytkettyä mikroaaltoavustusta. Mikroaaltosäteily on antennin avulla kohdistettu laser indusoituun plasmapalloon, jota se lämmittää ja pitkittää siten sen elinaikaa. Pidempi plasman elinaika mahdollistaa pidemmän signaalin integrointiajan, jolloin kerätty signaali paranee.

Tehdyissä tutkimuksissa antenniin kytketty mikroaaltoavustettu LIBS on on suoritettu ensimmäistä kertaa kiinteälle näytteelle normaalissa ilmanpaineessa. LIBS mittauksen herkkyyttä parannettiin 93 kertaisesti. Tämä paransi pienienergisellä laserpulssilla suoritetun mittauksen havaintorajaa 8.1 ppm asti. Koska antenniin kytketty mikroaaltoavustus osoittautui sekä tehokkaaksi että yksinkertaiseksi LIBS:n parannusmenetelmäksi, on sillä erinomainen potentiaali jatkokehityksen kannalta. Huolellisella antennisuunnittelulla sekä sen sijoittelun optimoinnilla siitä voidaan kehittää ratkaisu moniin eri teollisuuden ja tieteenalojen tarpeisiin.

PREFACE

This Master's thesis project was made in collaboration between Tampere University of Technology, Finland, and the University of Adelaide, Australia. It was supported by ARVI research program coordinated by CLEEN Ltd. and funded by Finnish Agency for Technology and Innovation, Tekes. I would like to thank Professor Zeyad Alwahabi for the ideas and guidance through the experiments and Doctor Juha Toivonen for feedback and supervision of writing the thesis.

I would also like to thank all the friends in Adelaide, who made it feel like home. Thanks also to the Optics lab people, especially to the past and present SK117A guys, and to the home support group called family.

Keep calm and focus harder.

Tampere, 29.7.2015

Jan Viljanen

TABLE OF CONTENTS

1. INTRODUCTION

Multiple fields of industry and science requires sensitive, fast and reliable elemental detection. The current methods e.g. in mineral analysis: chemical analysis; mass spectrometry; inductively coupled plasma atomic emission spectrometry (ICP-AES) do not exhibit all of these requirements. A possibility to monitor the elemental composition of a product in real time would greatly benefit industries, such as mining and steel industry, as separation of waste from the product would be more effective and classification of products would be easier. Latest development steps toward fulfilling the analytical needs described has been taken in the field of optical spectroscopy where Laser Induced Breakdown Spectroscopy (LIBS) has become a popular technique for elemental analysis. LIBS is an application of atomic emission spectroscopy, where the elemental analysis is performed on radiation emitted by a laser induced plasma. During last decade, LIBS has grown in to its own field of research with annual international conferences dedicated to it and growing number of publications published every year. [1, 2, 3] In this introductory chapter the needs of elemental analysis and the current solutions are described. Also the benefits of LIBS and the issues it could solve are introduced.

1.1 Elemental analysis needs and solutions

The needs of elemental detection in different targets and disciplines are vast. One of the recent hot topics has been the environmental analysis. Interest in aerosols, waste waters, resource conservation and sustainable agriculture has created great challenge to the elemental detection with great number of different measurement environments, conditions and sample types. Monitoring of the state of the environment requires elemental detection from soils, vegetatives, air and geological samples. Elements in interest vary also. Common elements in interest are the heavy metals due their toxic nature but also salts and nutrients, e.g. in the agricultural samples are under strict surveillance. [3, 4] Another constantly growing and challenging field

requiring elemental analysis is biomedical research. Trace element analysis of body fluids and soft tissues is used for pathological needs as well as toxicological analysis and on the other hand the mineral concentration of hard tissues are also under interest. Of course, in addition to environmental and biomedical needs, metal and energy industry has also needs of elemental analysis. The emissions, fuel quality, waste composition and product quality are under constant monitoring. [3]

As the problems and needs in elemental detection are various, so are the solutions. Multiple techniques and methods have been developed to meet the analysis requirements set by the different needs described. One of the most accurate and wide spread method is mass spectrometry. Mass spectrometric devices separate the input sample according to the mass of the sample particles and particles can be identified from the acquired mass spectrum. Mass spectrometry is extremely sensitive and can reach parts per trillion (ppt) level detection limits. By using mass spectrometry also isotopes can be separated. [5] Various methods for mass separation has been introduced with different characteristics. Maybe the most intuitively clear method is the time of flight (TOF) mass spectrometers in which charged sample particles are distinguished by using electric field and their time spent in the measurement chamber. [5] Other methods of mass spectrometry are sector instruments [6], quadrupole mass filter spectrometry [7] and ion trap mass spectrometry [8].

A successful method competing with mass spectroscopy is inductively coupled plasma (ICP) spectrometry and its variations. ICP can reliably reach parts per billion (ppb) level detection and therefore it has become the standard of many laboratories. [9] In ICP the powdered or fumed sample is turned into plasma with plasma torch and the characteristics of plasma are measured. The detection of the elemental composition is performed either by optical means from atomic emission (ICP-AES) or absorption (ICP-AAS) or by mass spectroscopical means (ICP-MS). [9, 10, 11] There are also lasers applied to the sampling of the sample. Sample is seeded to the plasma by using laser ablation (LA-ICP-AES/MS) when extremely fine sample particles are created. [12]

In addition to optical properties of elements, also interactions with more energetic radiation can be used to resolve the elemental composition of given samples. X-ray photoelectric spectroscopy (XPS) employs the photoelectrons induced by X-ray radiation. Elemental spectrum is gained by measuring the kinetic energy of released electrons.[13] For heavier atoms, such as lead (Pb) and mercury (Hg) XPS can

reach detection limits of ppb level but it has difficulties to detect atoms with atomic number of 5 or lower. Hydrogen (H) and helium (He) are practically impossible to detect by means of XPS. To reach good sensitivity, XPS also requires low pressure and sample preparation. Typically the elemental concentrations measured with XPS are in parts per thousand range. [14, 15] Also X-ray diffraction (XRD) is long known to be effective way to detect different elements and molecules. [16] X-rays propagate through the sample and diffracts from the lattices formed by the elements and molecules present. Different structures can be distinguished from the diffraction pattern formed to the detector. Also energetic radiation emitted by the sample can be used for elemental detection. By inducing neutron capture in the sample by bombarding it with a neutron beam, gamma radiation can be detected and the species present can be identified from the characteristics of induced radiation. This is called neutron activation analysis (NAA) [17, 18]

Elemental analysis can be performed also by chemical means, for example using sodium-fusion test [19] or oxygen flask method [20]. These methods are suitable for detection of elements in organic compounds and typically they are extremely specific. Specificity of chemical methods makes them usually slow and therefore analytical methods described earlier are much more common in practice.

None of the techniques described are perfect. All of them require sample preparation and therefore typically can only be performed in laboratory conditions. The sampling of the measured substance can also be slow and difficult which then affects to the overall efficiency of the method. Most of these methods are also relatively complex and therefore expensive. [2, 3]

1.2 Introduction to laser induced breakdown spectroscopy

Laser induced breakdown spectroscopy (LIBS) applies high irradiance provided by a pulsed laser source to create a plasma plume on a given sample. Radiation emitted from the plasma is detected and elements can be identified by analyzing obtained spectrum. Due the simplicity, LIBS has become an interesting option for various elemental detection applications. In addition to simplicity, LIBS possesses multiple great features desired for an analytical method. One of the most important of these features with which LIBS separates it self from other analytical techniques is that it requires no or minimal sample preparation. [3] This enables construction of stand-off capable devices. [21, 22] With simple, inexpensive and compact nature, LIBS

offers a solution to various quality control and trace element detection problems in different industrial targets. [3, 4] The stand-off capability and compactness has taken LIBS device even to Mars planet in the ride of the Mars rover. [22, 23]

LIBS's applicability is increased by the fact that it can be used on samples in any phase; liquid, gas and solid. Though, there is still challenges in liquid and solid sample measurements. [3] There has been few different methods introduced for liquid sample measurements. Straight forward solution has been to measure trace elements in water directly from bulk water. The performance of this approach is limited by the fast plasma cooling due the surrounding water environment. [24, 25] The cooling problem has been tried to avoid by measuring droplets [26] and avoided by drying the droplets before measuring the signal [4]. LIBS measurements on gaseous samples has been relatively successful and they are well established. Although, to achieve good results in gaseous samples a buffer gas may be required. Typical buffer gases for LIBS measurements are noble gases helium (He) and argon (Ar). [3, 27] Also aerosols and particles have been under LIBS studies. [28] In addition to elemental detection in aerosols, LIBS can be employed also for detection of aerosol mass and size distribution [29].

A vast application field for LIBS will be the elemental detection in solid samples. As mentioned in previous section, various disciplines require online, *in situ* measurements on solid targets. What hinders LIBS to become the standard of elemental detection, are the issues in quantitative analysis and the lack of sensitivity. Due the complicated laser-matter and plasma-particle interactions, shot to shot repeatability of signal is poor. This effect is called matrix effect due the multidimensional matrix of parameters on which the interactions depend. Also the sample matrix affects to the measurement and it is said that the calibration of LIBS measurement is one of the most difficult tasks to perform to achieve proper qualitative results. It is constantly stressed that for being able to calibrate LIBS signal, the calibration samples have to represent the actual sample matrix well. Therefore calibration has to be done separately for each measurement target which prevents the development of LIBS device for multiple targets. To overcome the need of calibration, calibration free (CF-LIBS) method has been introduced. [30] Not only the target, but also the measurement conditions have an effect to the measured signal. Temperature, pressure and gas composition of the ambient affects the signal. [3, 31]

As mentioned, LIBS falls behind its rivals especially in sensitivity. Typically LIBS

reach detection limit in parts per million (ppm) range while ICP and mass spectrometric techniques are capable to detect down to ppt level. The weak performance of LIBS in sensitivity is mainly due its nature as almost non-destructive measurement method. The used laser pulse ablates only a small amount of sample material and therefore also a very small amount of wanted target elements finds their way to the plasma and are possible to be detected. In fact, the absolute detection limit often translates into femtogram range. [32] There have been vast effort to improve the sensitivity of LIBS and various methods are introduced. These methods are further discussed in chapter 3. This thesis introduce sensitivity improvement of LIBS signal by applying microwave radiation to the laser induced plasma. By applying external energy to laser induced plasma, its lifetime can be prolonged. This enables longer signal integration times and improves measurement sensitivity. In chapter 2 the theoretical background of laser induced plasma is described. In chapters 4 and 5 the experimental arrangement and obtained results are discussed.

2. THEORETICAL BACKGROUND OF LASER INDUCED PLASMA

As soon as the pulsed laser was invented in the 1960, scientists found out its capability to induce plasma on surfaces. Since the first spectroscopical application of laser induced plasma in the mid 60's LIBS has developed into one of the most interesting spectroscopical methods with annual international conferences dedicated exclusively to it. [1] In this chapter the fundamentals of laser induced plasma formation and characteristics are described.

2.1 Light-matter interaction

Since the late 19th century, light has been know to be an electromagnetic disturbance in the form of waves which propagate through the ambient. The classical electromagnetism is beautifully summarized in a set of equations, known as Maxwell equations, formulated by James Clerk Maxwell. In the differential operator form and in the SI units they are

$$\nabla \times \boldsymbol{E} = -\frac{\partial \boldsymbol{B}}{\partial t}, \tag{2.1}$$

$$\nabla \times \boldsymbol{H} = \boldsymbol{J} + \frac{\partial \boldsymbol{D}}{\partial t}, \tag{2.2}$$

$$\nabla \cdot \boldsymbol{D} = \rho, \tag{2.3}$$

$$\nabla \cdot \boldsymbol{B} = 0, \tag{2.4}$$

where the electric field $\boldsymbol{E}$, the magnetic induction $\boldsymbol{B}$, the magnetic field $\boldsymbol{H}$, the electric current density $\boldsymbol{J}$, the electric displacement $\boldsymbol{D}$ and the electric charge density ρ are macroscopic time-dependent quantities. By applying presented Maxwell equations and using so called material equations

$$\boldsymbol{D} = \epsilon \boldsymbol{E}, \tag{2.5}$$

$$\boldsymbol{B} = \mu \boldsymbol{H}, \tag{2.6}$$

where ϵ is the electric permittivity and μ is the magnetic susceptibility, a wave equation can be derived. Differential wave equation for classical electromagnetic waves is

$$\nabla^2 \boldsymbol{E} = \epsilon\mu \frac{\partial^2 \boldsymbol{E}}{\partial^2 t}. \tag{2.7}$$

From wave equation, a wave function can be solved. The simplest case is a plane wave

$$\boldsymbol{E} = \boldsymbol{E_0} e^{i(\boldsymbol{k}\cdot\boldsymbol{r} - \omega t)}, \tag{2.8}$$

where $\boldsymbol{E_0}$ is the amplitude of the wave, $\boldsymbol{k}$ is the wave vector, ω is the angular frequency of the wave and t is time. Similarly, the wave function can be solved for the magnetic field of the electromagnetic radiation. In addition to the wave function, wave equation provides information also about the speed it propagates. The speed of light in medium v is defined as

$$v = \frac{1}{\sqrt{\epsilon\mu}}. \tag{2.9}$$

As seen from the eq 2.9, the speed of light depends only on the medium it propagates in. [33]

As the form of the electric field of the electromagnetic radiation can be solved, also

the average energy it carries per unit area per unit time can be calculated. This measure, called irradiance I, is defined as time average of squared electric field.

$$I = \epsilon v \langle \boldsymbol{E}^2 \rangle_t. \tag{2.10}$$

The electric field of the electromagnetic wave is the component which effectively exerts forces and therefore is more prone to interact with matter than the magnetic field. [33]

The main interactions between electromagnetic radiation and matter are scattering, which includes refraction, reflection and transmission, absorption, spontaneous emission and stimulated emission. Essentially the interaction depends on the relation between the matter and the radiation and it can be considered as a co-operative event between the electric field and the atoms in the matter. The interaction mechanisms depends strongly on the wavelength of the radiation. In the case of laser induced plasmas, the absorption of visible range radiation is one of the main forms of light-matter interactions. Interaction of short laser pulses with opaque material leads to the plasma production. Absorption of visible wavelengths happens usually through interaction between the radiation and the electrons. The absorption of radiation occur in a form of inverse Bremsstrahlung effect. Radiation is absorbed to the free electrons which act as seed electrons which then thermalizes the electron subsystem and heat the lattice. In non-metallic materials these seed electrons are usually from metallic impurities. The seed electrons then ionize the lattice and forms an avalanche effect where free electron number grows exponentially. When ultrashort pulses are used, multi-photon excitation can create free electrons even without metallic impurities and therefore absorption does not rely on them. As the number of electrons increase, eventually it reaches the critical electron density where irreversible damage to the matter occur and the growth of plasma begins. [34, 35]

In the scope of interest of this thesis is also the interaction between matter and electromagnetic radiation with longer wavelength. Microwave radiation is electromagnetic radiation in frequency range from 1 GHz up to 300 GHz which corresponds wavelengths from 30 cm to 1 mm. Interaction between microwave radiation and matter is slightly different from the interaction between visible light and matter. Microwave radiation also interacts with free charged particles if they are present in the target matter but, due much shorter atomic and electronic depolarization times

than the microwave oscillation period, this process does not contribute to the lattice heating. Due lower frequency of electric field oscillation, microwave radiation can interact with molecules possessing dipole moment and induce dielectric polarization to dielectric lattices. The dipoles rotate to align themselves with the oscillating electric field which then contributes to the heating of the material. [36] However, in absorption of microwave radiation to plasma there is also other mechanisms. As microwave radiation propagates through plasma plume, it accelerates charged particles as its electric field oscillates. This acceleration causes collisions between the particles present in the plasma. Energy of microwave radiation is absorbed by electron-ion and electron-neutral collisional absorption. The electron-neutral collisional absorption is estimated to be the most significant method of microwave absorption in a plasma plume. A contribution to the microwave absorption is also given by number of instabilities in the plasma. [37]

2.2 Laser induced plasma formation on solids

Plasma is the fourth fundamental state of matter. It is a local assembly of atoms, ions and free electrons. Plasma can be characterized by multiple parameters. The most basic one is the degree of ionization i.e. the ratio of free electrons to other particles. Laser induced plasmas typically fall into category of weakly ionized plasma in which less than 10 % of the species are free electrons. [1, 38]

As plasma is extremely energetic form of matter, for laser being able to induce plasma on sample, the irradiance of the laser beam should exceed a certain threshold value. Typically these threshold values are in the order of few GW cm^{-2} to hundreds of GW cm^{-2}. Threshold values vary from sample to sample and they are also wavelength and pulse width dependent.[1, 39] These threshold values set certain requirements for the laser selection. To achieve the required irradiance on the sample surface a pulsed laser is mandatory. Pulsed output beam is also focused by focusing lens to increase the irradiance above the threshold.

The formation and evolution of laser induced plasma is schematically presented in Fig 2.1. The leading edge of the laser pulse interacts with the sample surface heating, melting and vaporizing it. This creates an ablation fume consisting sample particles and vaporized sample above the sample surface. This process is called laser ablation. As ablated material is still in atomic state, i.e. has not reached the plasma state, part of the laser pulse still goes through the fume and continues interaction with the

sample. The minimum irradiance I_{min} required to ablate material can be estimated by equation

$$I_{min} = \rho L_v \kappa^{1/2} / \Delta\tau_p^{1/2}, \tag{2.11}$$

where ρ is the density of material, L_v is the latent heat of vaporization, κ is the thermal diffusivity of the sample and $\Delta\tau_p$ is the width of the laser pulse. Ablation is a complex phenomena which depends on a multidimensional matrix of parameters. After ablation an ablation crater is left. Depending on the laser pulse characteristics, ablation can remove from ng to μg of sample matter. [1, 2]

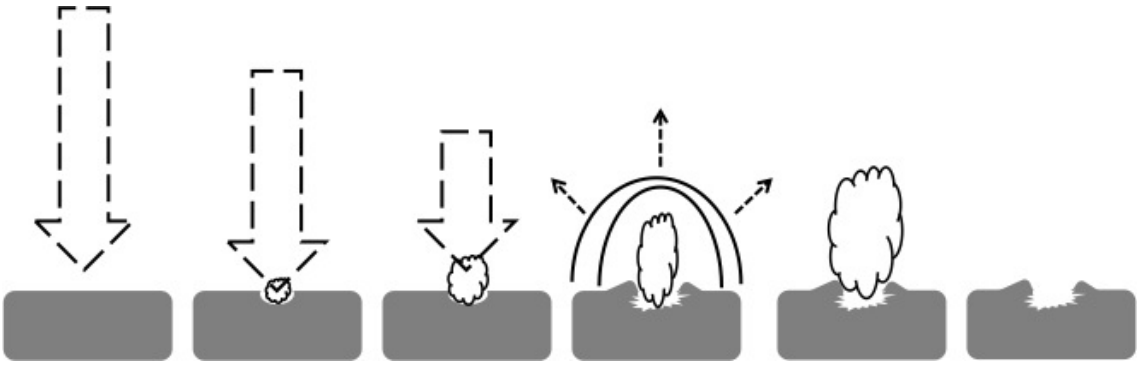

Figure 2.1 *Plasma formation on solid sample. Dashed arrow represents the laser pulse which first ablates the sample and then ignites the plasma.*

As the leading edge of the laser pulse has ablated the sample, part of the pulse energy starts to heat the ablated material. When laser pulse has high enough energy, it can heat the plasma so that it becomes opaque to the laser beam. At this state, sample surface is shielded by the plasma and laser beam does not reach the sample any more. All the energy in the remaining laser pulse absorbs to the plasma shield and plasma starts to grow towards the direction of incoming beam. Opaque state of plasma occur when the energy density exceeds the critical electron density n_c

$$n_c \sim (10^{21}/\lambda^2)/cm^3, \tag{2.12}$$

where λ is the laser wavelength in microns. [1] As plasma is formed it starts to expand. At initial conditions of plasma, beginning of the expansion and close to the sample surface, the plasma may be considered to be in local thermal equilibrium

(LTE). However, this cannot be assumed further than the extent of the laser pulse. [40] At first, the plasma plume expands adiabatically acting as a piston to the ambient gas. Ambient gas is heated and compressed creating an external shock wave. This shock wave decelerates and reheats the plasma. Counter pressure from ambient gas creates an internal shock wave to the plasma which homogenizes it and forms most of the internal energy into thermal form. At this stage, expansion is not adiabatic anymore and plume pressure, particle velocity and temperature decreases. Eventually plasma has lost all its energy and dies out. [41] The external shock wave can be acoustically detected as a loud noise as the shock front propagates through the ambient.

2.3 Fluorescence radiation from laser induced plasma

Laser induced plasma emits electromagnetic radiation. Radiation emitted can be classified into three different categories according to its origin. The first category is radiation emitted from bound-bound transitions. Due thermal excitation, a bound electron on quantum state l is excited to a higher quantum state u, still remaining bound in an atom. As the excitation relaxes back to the original state radiation is emitted with energy E_ν so that

$$E_\nu = E_u - E_l = h\nu_{ul} = \frac{hc}{\lambda_{ul}}, \tag{2.13}$$

where E_l and E_u are the energies of lower and upper quantum state, respectively, h is the Planck's constant, ν_{ul} is the frequency of the radiation emitted from the transition and λ_{ul} is the corresponding wavelength and c is the speed of light. An example of a simple atomic energy level structure is given in Fig 2.2 The frequency is characteristic to each transition in each atom and ion. The frequencies from bound-bound transitions extend from the near-infrared (NIR) to ultraviolet (UV) part of the electromagnetic spectrum. This characteristic radiation can be used to recognize the elements in the plasma. [38]

The second category of plasma emitted radiation is radiation originated from free-bound transitions. In free-bound transition a free electron is recombined with an ion. As kinetic energy of free electrons may be assumed non-quantized, the radiation from free-bound transitions has continuous spectrum. The electron's excess kinetic energy $E_k = 1/2 m_e v_e^2$ is contributing to energy of radiation according to relation

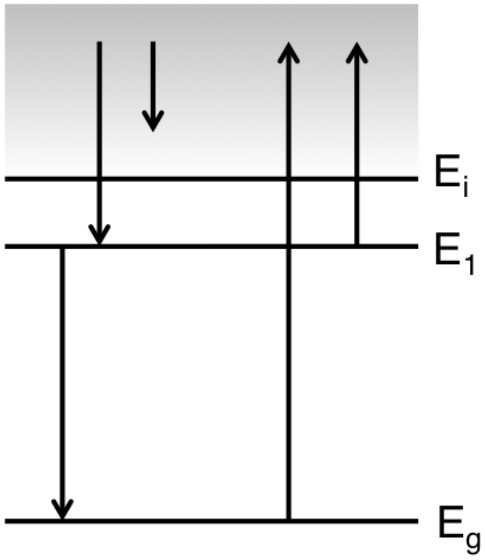

Figure 2.2 *Schematic illustration of atomic energy levels and possible transitions. Transitions from left to right: bound-bound, free-bound, free-free, ionization from ground state and ionization from exited state.*

$$E_\nu = E_k + E^I - \delta E - E_u = h\nu, \tag{2.14}$$

where E^I is the ionization energy of corresponding ion, δE is its lowering and E_u is the energy of the state to which the electron is trapped. Due electrons spreading to large spectrum of energies recombination to level u will provide to scale of spectrum from ν_{min} to large values of ν. Another category which contributes to continuous radiation of plasma is the free-free transitions. Free electrons in the plasma loose part of their kinetic energy in the collisions with ions. The lost energy is emitted as continuum radiation called bremsstrahlung. Bremsstrahlung is typically in the IR part of electromagnetic spectrum. In laser induced plasma the continuous spectrum of the radiation is dominant approximately during first 100 ns of plasma lifetime. The continuum decays much faster than the emission from bound-bound transitions and therefore when laser induced plasma radiation is detected the early stage of the plasma is tried to be avoided by delaying the measurement. The evolution of plasma fluorescence is schematically described in Fig 2.3. [1, 38]

The main source of information of plasma properties is the line emission from bound-

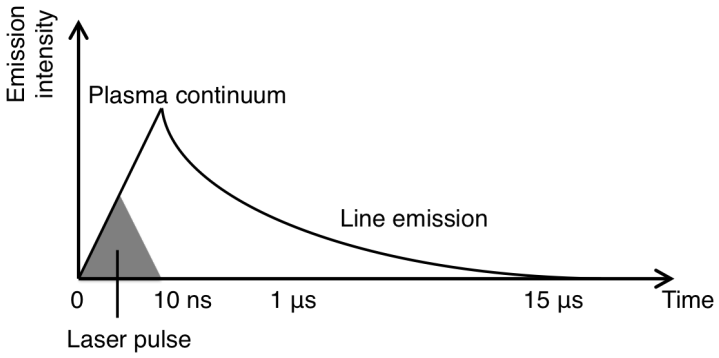

Figure 2.3 *Example of temporal plasma fluorescence evolution and dominant spectral features.*

bound transitions. From characteristics of the line shape the element, electron temperature and electron density can be determined. The recognition of the element can be done from the central frequency of the emission line by comparing it to a database of elemental lines. The calculation of other two properties is also relatively simple but requires understanding of the line broadening mechanisms. All atomic lines exhibit natural broadening due the uncertainty principle $\Delta E \Delta \tau \geq \hbar$, where ΔE is the width of the corresponding energy level, $\Delta \tau$ is its lifetime and $\hbar = h/2\pi$. As natural broadening is homogeneous broadening mechanism, the line shape due it can be described with Lorentz expression

$$\Gamma_L(\nu) = \frac{1}{2\pi} \frac{\Delta\nu_H}{(\nu - \nu_0 - \Delta\nu_V)^2 + (\Delta\nu_H/2)}, \tag{2.15}$$

where $\Delta\nu_H$ is the full frequency width at half maximum, $\Delta\nu_V$ is the frequency shift of the line in relation to unpertubed line maximum ν_0. Contribution of natural broadening to line shapes emitted by laser induced plasmas is small compared Doppler and Stark broadening and can therefore be neglected when such emission lines are considered. [1, 38, 42]

The Doppler broadening is inhomogeneous broadening mechanism which of width depends only on the temperature T and mass M_a of emitting species. Emission lines exhibit Doppler broadening due the velocity distribution of the emitting species. The inhomogeneous line profile can be described with Gauss function

$$\Gamma_D(\lambda) = \frac{1}{\Delta\lambda_p \pi^{1/2}} \mathrm{e}^{\left[-\left(\frac{\lambda-\lambda_0}{\Delta\lambda_p}\right)\right]}, \tag{2.16}$$

where

$$\Delta\lambda_p = \lambda_0 \left(\frac{2kT}{mc^2}\right). \tag{2.17}$$

From the equation 2.16, the full width half maximum (FWHM) of the line shape can be solved as

$$\Delta\lambda_D = \left(\frac{8kT\ln 2}{M_a c^2}\right)^{1/2} \lambda_0, \tag{2.18}$$

where k is the Boltzman's constant and $\lambda_0 = c/\nu_0$ is the central wavelength of corresponding emission line. [1, 38, 42]

Collisions between charged particles in the plasma cause Stark broadening. This, so called Stark effect, degenerates sublevels identified by quantum number m_j which leads to either unresolved broadened line profile or a resolved series of sublevels. Stark broadening is homogeneous broadening mechanism which depends mainly on electron density n_e and it becomes dominant when the ionization ratio becomes greater than 1%. The line width $\Delta\lambda_S$ (FWHM) of Lorentz function 2.15 for neutral atoms can be solved as

$$\Delta\lambda_S = \left[1 + 1.75A\left(1 - \frac{3}{4}N_D^{-1/3}\right)\right] W_{FWHM}\left(\frac{n_e}{10^16 cm^{-3}}\right), \tag{2.19}$$

where A is the dimensionless coefficient, N_D is the number of particles in the Debye sphere and W_{FWHM} is the Stark broadening parameter. If the ionic part is neglected, relation 2.19 is reduced to

$$\Delta\lambda_S = W_{FWHM}\left(\frac{n_e}{10^{16} cm^{-3}}\right) \tag{2.20}$$

which can be used to determine the electron density.

In general, broadening of line emission is combination of Doppler and Stark broadening mechanisms. The resulting line shape is described by Voigt profile which is convolution of Gauss and Lorentz functions as follows:

$$\Gamma_V(\lambda) = \frac{2\sqrt{\ln 2/\pi}}{\delta\lambda_D} K(u,a). \tag{2.21}$$

The $K(u,a)$ is known as Voigt function

$$K(u,a) = \frac{a}{\pi}\int_{-\infty}^{\infty} \frac{\mathrm{e}^{-t^2}}{(u-t)^2+a^2}\mathrm{d}t, \tag{2.22}$$

where the variables u and a are

$$u = \frac{2\sqrt{\ln 2}}{\Delta\lambda_D}(\lambda - \lambda_0), \tag{2.23}$$

$$a = \sqrt{\ln 2}\frac{\Delta\lambda_S}{\Delta\lambda_D}. \tag{2.24}$$

By fitting a Voigt profile to measured emission line the plasma parameters can be determined. The Gauss, Lorentz and Voigt profiles are plotted in Fig 2.4. One can see how Gauss profile is dominant at close to the line center and Lorentz profile in the wings of the line. [1, 38, 42]

Usually, the line shape is not ideal due self absorption. Self-absorption occur when inside the plasma the line emission is absorbed by the same species as the emitters. This is unavoidable since if there is emission from quantum level u to level l it means that there is population present at level l that can absorb the radiation and be excited back to level u. Self-absorption is strongest in ground level transitions since the ground level of atom is always populated in laser induced plasmas. An example line shape of self-absorbed line is shown in Fig 2.5. Sensitiveness of a line for self-absorption can be estimated by factorizing the absorption coefficient $\alpha(\lambda)$

$$\alpha(\lambda) = \Gamma(\lambda)N_a^z k_t, \tag{2.25}$$

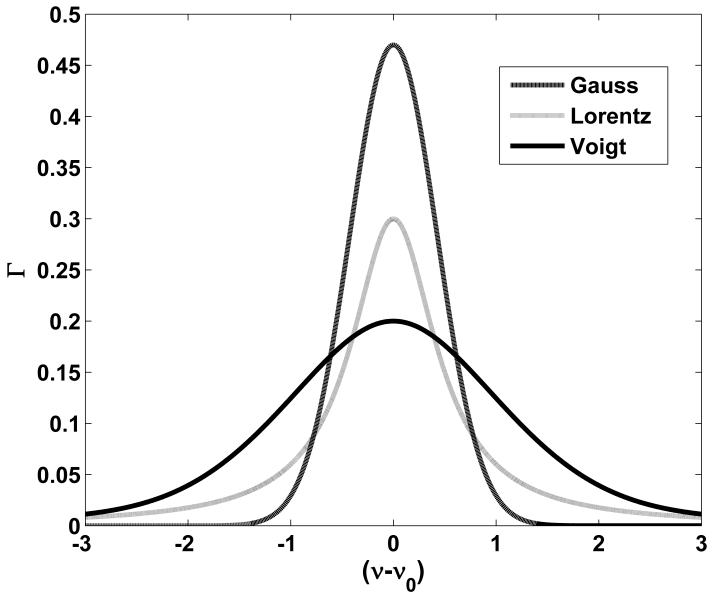

Figure 2.4 *Plot of Gauss, Lorentz and Voigt profiles.*

where N_a^z is the density of ion species at charge z and k_t is a quantity which depends only on the atomic data and the temperature as follows: [42]

$$k_t = \frac{e^2}{4m_e c^2 \epsilon_0} f_{ij} \lambda^2 \frac{g_i}{u_a^z(T)} \mathrm{e}^{-\frac{E_i}{kT}} \left(1 - \mathrm{e}^{-\frac{hc}{\lambda kT}}\right). \tag{2.26}$$

In equation 2.26 e is the elementary charge, m_e is the electron mass, ϵ_0 is the vacuum permittivity, f_{ij} is the oscillator strength, g_i is the statistical weight of initial level, $u_a^z(T)$ is the partition function of species a and E_i is the energy of the initial level. Plasma is called optically thick when absorption of light propagating through it is prominent. [42]

2.4 Quantitative analysis and analytical figures of merit

Due the characteristic radiation emitted by the laser induced plasma, qualitative elemental detection is relatively easy to perform. This requires recording of the emission spectrum and recognition of emission peaks. Quantitative analysis requires sensitive resolution of the peak intensities. Due complex nature of light-matter interaction and plasma formation emission intensities vary greatly from shot to shot.

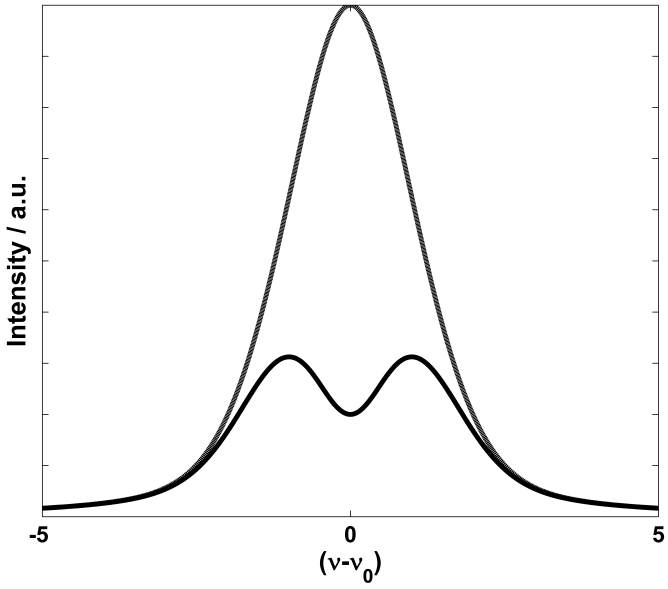

Figure 2.5 *An example of self-reversed line profile due self-absorption.*

These defects depends on a multidimensional matrix of parameters and therefore they are called matrix effects. [1, 3] Matrix effects lead to a lack of shot to shot repeatability which is the main reason of difficulties in quantitative LIBS. Measurement repeatability is described by term precision. It is a measure how well a set of measurement results x_i agrees with them selves. Usually precision is expressed as deviation of a set of measurements n from arithmetic mean M of the set of repeated measurements. The deviation can be calculated as standard deviation

$$std = \left[\frac{\sum(x_i - M)^2}{n-1}\right]^{1/2}. \tag{2.27}$$

Typically, to improve the precision in LIBS measurement many individual spectra are collected and they are used to produce average measurement. To produce replicate measurements the measurement conditions are kept constant and multiple an average measurements are collected. The number of shots collected to form an average depends on the measurement parameters: Sample homogeneity, sampling method, required duty cycle and desire to maximize the performance. Number of averaged pulses vary from tens to thousand laser pulses. [1]

To perform quantitative LIBS measurements, a calibration curve of instrumental response versus the elemental concentration of sample needs to be measured. It is often expressed that the calibration is the most difficult issue in the development of LIBS. The necessity of using calibration samples with the same or at least similar sample matrix is often stressed. However, calibration curves are constantly produced to perform quantitative analysis and compare the analytical performance. There are various types of calibration standards commercially available or they have to be self-produced by, for example, adding known amounts of analyte to pure samples. Ideally a calibration curve is linear and passes the origin but typically, when they are extended to a broad concentration scale, they exhibit square root behavior. Linear part close to the origin can be used to define the sensitivity of the measurement system. By fitting a linear fit to the measured data points the slope of the concentration to intensity function can be solved. The calibration slope at certain concentration is termed as sensitivity. It is the change in signal for a given change in concentration. As mentioned, the sensitivity varies when moving from low concentrations to high concentrations. The decrease in sensitivity in high concentration samples is mostly due self-absorption. The changes of sensitivity in low concentration samples can be due to spectral interferences, constant background concentrations or incorrect determination of the analyte signal. [1, 3]

The slope of calibration curve can also be used to determine the limit of detection LOD. The limit of detection is defined as the concentration c_L derived from the smallest measure x_L that can be detected with the given analytical procedure and

$$x_L = x_{bi} + ks_{bi}, \tag{2.28}$$

where x_{bi} is the mean of blank measurements, k is a numerical factor chosen according to confidence level desired and s_{bi} is the standard deviation of blank measurements. From here an expression for LOD can be derived as

$$LOD = \frac{ks_{bi}}{b}, \tag{2.29}$$

where b is the slope of the linear part of calibration curve. [1, 3]

The ability of a measurement procedure to give "true" values is termed accuracy.

Accuracy tells how close the measured value is to the actual concentration contained by the sample. The problem with defining the accuracy is that a method for defining the absolute true value does not exist and therefore the comparison has to be done with accepted true value x_{atv}. The error x_{err} of measured value x_m is defined as the difference from the accepted true value

$$x_{err} = x_m - x_{atv}. \tag{2.30}$$

The inaccuracy, i.e. the error, may be classified in two categories by the type of occurrence: systematic error and random error. Systematic error is an error which appears in measured values as systematic shift away from the true value. This is often due some error in measurement procedure such as miss-alignment or mistuned laser. Random error raises usually from more fundamental aspects of the measurement system and therefore it cannot be avoided. For example, laser pulse energy may fluctuate randomly or minor variation on the sample surface may change the ablation conditions. The effect of random error can be diminished by averaging over large number of laser pulses. [1]

3. LASER INDUCED PLASMA FLUORESCENCE SIGNAL ENHANCEMENT TECHNIQUES

With many advantages over other analytical techniques, LIBS offers interesting solution to multiple elemental detection needs. The main limitations for LIBS to become the standard practice in all instances requiring elemental analysis are the difficulties in quantitative analysis and the lack of sensitivity. There has been vast interest to improve these weaknesses and great effort in form of applied LIBS techniques has been seen. This chapter describes a few unconventional LIBS techniques developed to overcome the limitations in sensitivity of conventional LIBS.

3.1 Spatial confinement of laser induced plasma

When LIBS signal is measured, the acquired signal comes from limited spatial volume. The collection volume is limited by the collection lens, which seldom covers the whole laser induced plasma. In spatial confinement of laser induced plasma, the expansion of plasma is prevented by obstacles or magnetic field. By preventing the plasma expansion the plasma is spatially positioned to the optimal location for signal collection and the radiation emitted from the whole plasma can be collected. This increases the signal collection efficiency and therefore the sensitivity is improved. This is relatively simple and inexpensive method to improve LIBS sensitivity.

To accomplish the spatial confinement of laser induced plasma, few different techniques has been introduced. The simplest case is to limit the plasma expansion by inducing it into a cavity which is sown in Fig 3.1. Different cavity geometries are studied. A simple cylindrical chamber [43, 44] is simple and easy way to achieve sensitivity enhancement factors from 2 to 10 depending on the element. The drawback of cylindrical cavity is the free expansion axis to the direction of laser. This has been tried to minimize by hemispherical cavity geometry. [45, 46] Hemispherical

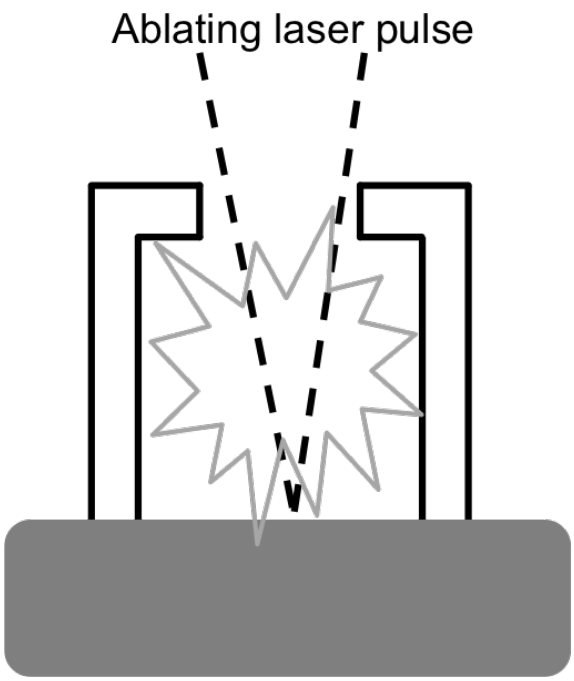

Figure 3.1 *A schematic example of cavity spatial confinement of laser induced plasma*

cavity did not improve the sensitivity much compared to cylindrical cavity but the linearity of calibration curve slightly improved and therefore improved the methods applicability to quantitative analysis. Another approach to spatial confinement has been using magnetic field to prevent the plasma expansion. [47] Magnetic field is applied to the plasma which then expands across it. Magnetic field spatial confinement of laser induced plasma with magnetic field of 0.8 T improved the sensitivity by factor from 2 to 8. By combining the cavity and magnetic confinement enhancement factor of 24 was achieved. [48] Spatial confinement has also been combined with enhancement techniques introduced in following sections. Combination of two-wall spatial confinement and double pulse LIBS achieved 168 fold improvement to LIBS sensitivity which is good even compared to double pulse arrangement alone which gave 106 fold improvement. [49] Spatial confinement combined to spark discharge assisted LIBS improved the sensitivity but also pulse to pulse repeatability. Spatial confinement was seen to stabilize the plasma morphology which explained the improved repeatability. [50]

3.2 Double pulse laser induced breakdown spectroscopy

One of the most studied and applied unconventional LIBS technique is double pulse LIBS (DP-LIBS). The aim with DP-LIBS is to increase the signal intensity through better coupling of laser energy to ablated material. Better coupling will lead to more efficient production of analyte atoms in excited state. Several double pulse configurations have been demonstrated and it has been found that DP-LIBS is a possible approach to improve the analytical capabilities of LIBS. [1, 3, 51]

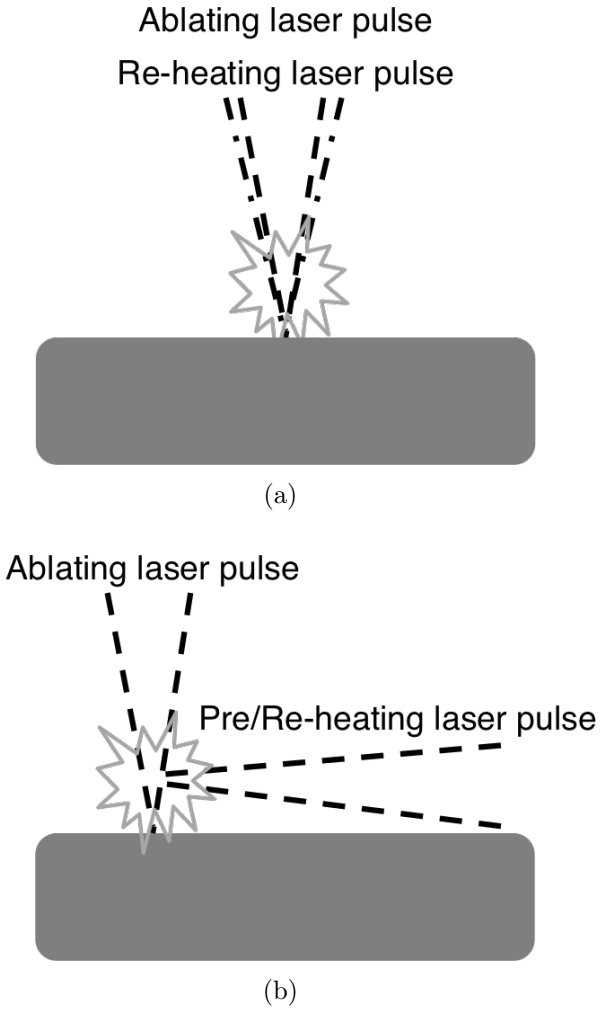

Figure 3.2 *Schematic representation of a) collinear and b) orthogonal double pulse LIBS*

Geometrically the two pulses have been mainly combined with two different orientations: collinearily and orthogonally. The two configurations are represented in Fig 3.2. In collinear beam configuration both pulses have the same axis of propagation.

The first pulse is set to create the ablation and ignite the plasma. As the second pulse will be timed ∼1 μs after the first pulse, it will be absorbed to the plasma. Absorbed second pulse will reheat the plasma and improve the analytical sensitivity. For collinear configuration an improvement factor of 2 up to 100 has been reported. In the orthogonal configuration the other pulse propagates parallel to the sample surface. Orthogonal configuration can be used similarly to collinear for reheating the plasma but also pre-ablation is possible. In pre-ablation the pulse parallel to surface is focused above the intended ablation spot and it creates an air plasma. This then improves the plasma emission from the second pulse. An improvement factor of 7 to 33 has been reported for orthogonal DP-LIBS. [1, 51, 52, 53]

In addition to variation of geometry also other parameters can be varied. The two laser pulses can be produced either with the same laser or two different lasers. Use of two lasers allows combination of pulses with different characteristics: pulse duration, wavelength and energy. One of the best improvement factors have been gained with combining 1064 nm Nd:YAG pulse with simultaneous 10.6 μm CO_2 laser pulse. The factor of 25 up to 300 improvement of signal intensity was observed depending upon the emission line. [51, 54, 55]

With DP-LIBS, several ablation parameters such as electron density and temperature, crater volume, ablation efficiency and emission intensity can be improved. Decreasing crater depth means that less damage is caused to a sample. Practically this is possible by using lower laser pulse energies which the signal improvement by DP-LIBS enables. This is important when there is small amount of sample available or an art piece which is not wanted to damage is measured. DP-LIBS suffers from the fact that the decreased crater depth and improvement of LOD cannot be achieved with the same measurement parameters. This forces the parameters to be chosen to match the application and compromises has to be done. [3, 51]

3.3 Spark discharge assisted laser induced breakdown spectroscopy

A similar technique to DP-LIBS to improve LIBS sensitivity is spark discharge assisted LIBS (SD-LIBS). Instead of an another laser pulse, an electrical spark discharge is used to deposit more energy and reheat the plasma. The laser pulse is focused through tungsten alloy electrodes on sample surface. Typically the distance from the electrodes capable to carry voltages of ∼10 kV to sample surface is ∼2 mm.

Spark discharge is launched as the laser induced plasma reaches the electrode gap. Due the electrons provided by the plasma, a discharge can be produced with lower voltage than without the initial laser induced plasma. The voltage required depends on the laser pulse energy used. As low voltages as 0.5 kV can be used to enhance the laser ignited plasma when laser power is sufficiently high. With SD-LIBS, signal intensity enhancement factor of 50 up to 400 depending on the laser fluence has been achieved.[56, 57]

Great improvement of sensitivity has enabled the use of low laser pulse powers without compromising the sensitivity. This causes less damage on the sample surface still providing detailed information of the elements in interest. SD-LIBS has also been observed to stabilize the shot to shot fluctuations of conventional LIBS signal. This would improve the accuracy of quantitative analysis. Despite the promising results gained with SD-LIBS it has not become common practice. [3, 56] This might be due the high voltage required for the spark discharge production. Spark discharges also function at relatively low frequency of $\sim$1 Hz[56] which slows down the experiment significantly. This might limit also the choice of laser and increase the expenses of the experimental setup.

3.4 Flame assisted laser induced breakdown spectroscopy

A LIBS method where a flame is set near the ablated sample surface has been introduced. [58] An oxygen-acetylene flame, being a plasma itself, is set close to a sample surface. Laser induced plasma is generated in the blue outer envelope of the flame having temperature of 1200 °C. Flame therefore acts as a pre- and re-heating component. This has shown improvement of the signal intensity and narrowed the spectral line width. The main factor of flame enhancement is the increased plasma temperature in the early state of plasma evolution which produces more excited atoms. Also the evolution of plasma is affected and as a result high temperature but low electron density plasma is produced. Reported 4-fold enhancement to the signal and 60 % narrower signal implies improved spectral resolution and sensitivity.

More simple and cost effective solution for pre-mixed stable flame is to use commercial micro torch to provide the heating component. [59] Similarly to the previous case, the laser pulse is shot to the outer envelope of the flame. Signals from low concentration elements in steel samples, such as aluminum (Al), manganese (Mn) and vanadium (V), were enhanced approximately 5 times compared to conventional

LIBS. This improved the limit of detection, for example, in the case of Mn from 425 ppm to 139 ppm.

3.5 Microwave assisted laser induced breakdown spectroscopy

Using microwave radiation to reheat the laser ignited plasma has produced promising results. When the electron density of the plasma decreases to a level which is lower than critical electron density for microwave radiation, the plasma does not act as a mirror to the radiation anymore. For microwave radiation at 2.45 GHz frequency the critical electron density is 7×10^{10} cm^{-3}. Microwave assisted LIBS relies on the coupling of the low density plasma and the microwave radiation. As noted in section 2.2, the initial electron densities are in the order of 10^{21} cm^{-3}, but as the plasma relaxes and in its periphery the electron density will decrease below the critical value. [60, 61]

There are two main techniques to deposit the energy of microwave radiation to the plasma: microwave cavity and microwave antenna. A technique in which plasma is exposed to microwave radiation by igniting the plasma inside a microwave cavity has produced even a commercial product. [62] Microwave assisted LIBS system LAMPS has been launched by Ocean Optics and it has gained some popularity among researchers. In LAMPS, a sample is set inside a microwave cavity which has a window for laser pulse. Laser pulse then ablates the sample and ignites the plasma. Applied microwave prolongs the plasma lifetime and therefore improves the sensitivity of LIBS measurement. Depending on emission line and sample type enhancement factors of 10 to 1000 has been achieved. Microwave cavity enhancement has been applied to several different sample cases. [60, 62] Microwave cavity has also been applied to improve the sensitivity of LIBS measurements on low copper concentration samples. 23-fold improvement of the sensitivity was achieved in soil sample analysis. [63]

In antenna-coupled microwave case, instead of putting the sample inside a cavity, the microwave radiation is brought to the sample by an antenna. Gas phase analysis has been done with using conical shape tip antenna. Antenna is set 5 mm away from the laser focal spot where the plasma is ignited. Radiation emitted from the antenna prolongs the plasma lifetime with the same mechanism as in the microwave cavity. Enhancement factor of 15 has been achieved in the intensity of LIBS spectra of air in atmospheric pressure.[61, 64] Antenna-coupled microwave assist has been

applied also to solid samples. Helical antenna is brought close to the sample and the plasma is ignited to the center of the loops. To gain enhancement in the case of solid samples, a vacuum chamber has been used. At low pressure, 50-fold improvement of LIBS sensitivity has been observed. At atmospheric pressure, no or negligible enhancement effect was found. [65, 66]

4. EXPERIMENTAL ARRANGEMENT

The experiments for this thesis were conducted in the School of Chemical Engineering, University of Adelaide. In this chapter, the details of the experimental setup are presented and the experimental procedure is discussed.

4.1 Laser, spectrometer and measurement geometry

The schematic description of the measurement setup used in the experiments is given in Fig 4.1. For ablation and plasma ignition a Q-switched frequency doubled Nd:YAG laser (Continuum Surelite II) was used. The repetition rate of the 532 nm wavelength laser pulse was 10 Hz and the pulse width was approximately 10 ns. The maximum output energy of the laser was 180 mJ which was used to maintain stable lasing from the laser head throughout the measurements. The laser pulse energy was then reduced with a half-wave plate and a polarizer cube. The energy used for plasma formation was monitored with power meter. Due the high energy of pulses used, steering of the laser beam was done with 532 nm laser line high damage threshold dichroic mirrors (Thorlabs). Laser was focused on the sample surface with a UV-fused silica lens with 100 mm focal length. This produced spot size of approximately 100 μm at the focal distance. Sample surface was chosen to be placed at the focal distance from the focusing lens to achieve good consistency to the sample to lens distance and optimal detection efficiency with the detection method used.

Collection of the fluorescence radiation from the plasma was done with the same lens as the focusing of the laser pulse. The laser pulse was steered to the lens with a dielectric mirror. The dielectric mirror had high reflection at 500 - 550 nm but good transmission in the shorter visible wavelengths which were in the scope of interest. The extinction spectrum of the mirror is plotted in Fig 4.2. After transmission through the dielectric mirror, the fluorescence radiation was focused to an optical fiber for transportation to the spectrometer. Collection method used was compared

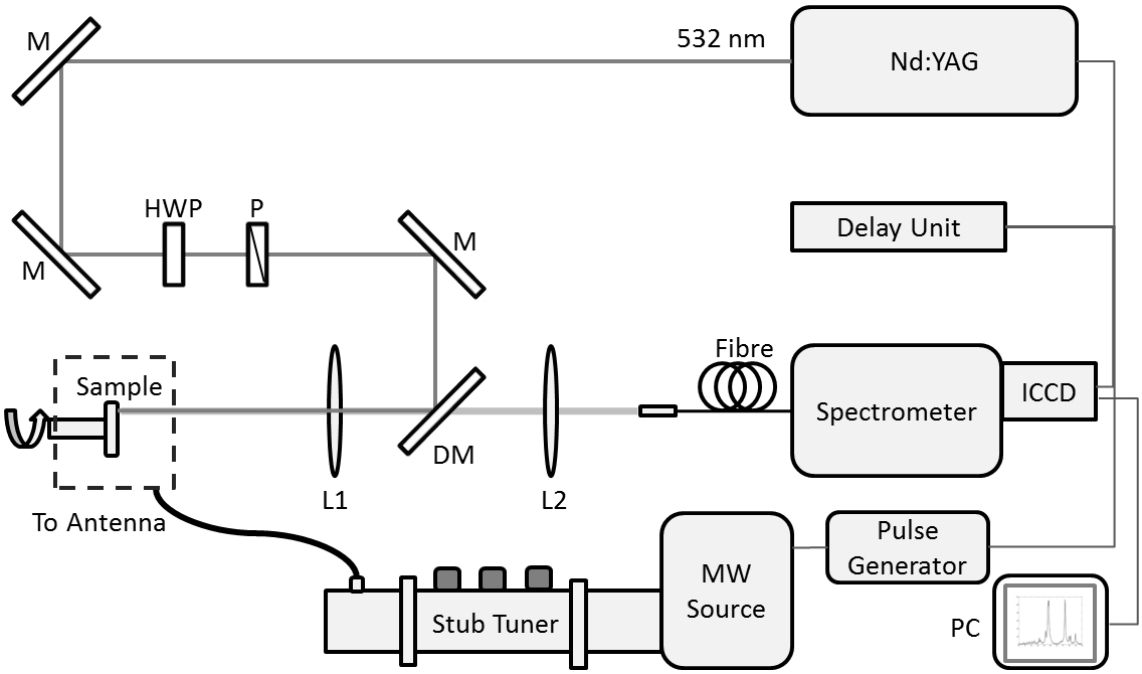

Figure 4.1 *Schematic illustration of the measurement setup*

to a more traditional collection method where a separate collection lens is used for signal collection. The latter method requires much more careful alignment and is more vulnerable for sample misplacements than the method chosen to use in the performed measurements. With careful alignment, both methods presented similar efficiency and measurement results were not dependent on the collection geometry.

Spectrometer (Andor Shamrock 500i), used to resolve the spectral features of the fluorescence signal, was equipped with two different gratings. For low resolution measurements a grating with 150 l/mm was used. To obtain more detailed information of the fluorescence spectrum, high resolution measurements were performed with a grating having 600 l/mm. At the output of the spectrometer was placed an intensified charge-coupled device (ICCD) camera (Andor iStar). This allowed accurate adjustment of gate delay and gate width of the detection. Fluorescent light from plasma was transported to the spectrometer with an optical Y-shaped optical fiber bundle (Thorlabs, BFY400HS02) having 19 high OH fiber cores with diameter of 200 μm. The Y-shaped fiber bundle was chosen for easy transition between the two different signal collection methods. Light was transmitted to spectrometer through a slit having width of 5 μm. Narrow slit was chosen to achieve high spectral resolution, although, it leads to high losses of light. Due good collection efficiency

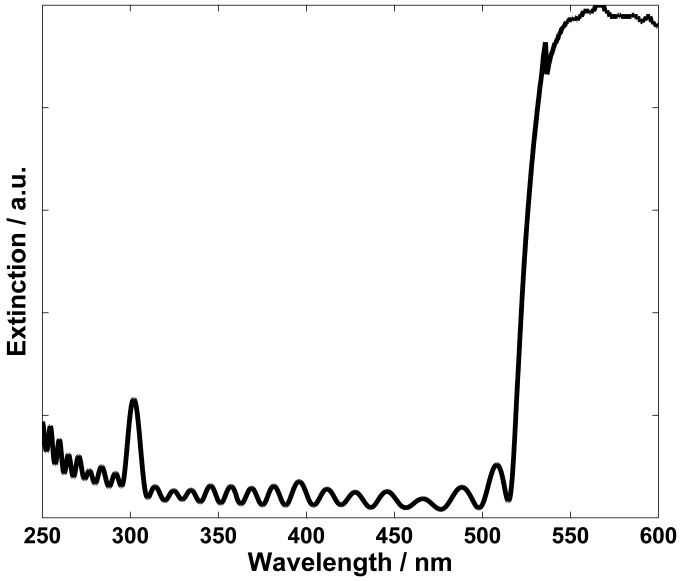

Figure 4.2 *Extinction spectrum of dielectric mirror used for laser beam steering and signal collection.*

of fiber bundle used, the losses were tolerable.

4.2 Microwave source

Microwave source used to create the microwave (MW) pulses for LIBS signal enhancement was magnetron microwave generator (Sairem) with frequency of 2.45 GHz and maximum output power of 3 kW. The source had both continuous wave (CW) and pulsed modes. Pulsed mode was used in the experiments to avoid overheating the antenna. The magnetron generated the MW radiation in to a wave guide. To wave guide, a 3-stub tuner was connected to match the impedance of the wave guide to the connected antenna cable. Transition from wave guide to coaxial antenna cable was done with special waveguide to coaxial coupling component. By adjustment of the tuner, a 70 % coupling efficiency from wave guide to the antenna cable was achieved. This was measured by following the output radiation power and back reflected radiation power. Due the high powers present inside the MW source, it required water cooling.

The microwave source was driven with external pulse generator (Aim-TTi) to obtain accurate control of MW pulse timing, power and width. Pulse generator fed the MW

source with square wave of which amplitude determined the peak power of the MW pulse and the width of the square wave determined the width of the MW pulse. MW source had its own rise and fall times which had to be considered. The typical rise time was 100 μs and fall time 200 μs.

To ensure the safe use of the microwave source, leaked MW radiation was constantly monitored. The source and waveguide was found to be well sealed and only source of MW radiation to the surrounding was the antenna. Radiation from the antenna stayed within the safety limits over 20 cm away from the antenna. The MW was turned off every time a sample or the antenna was handled to prevent radiation exposure. To minimize the microwave radiation from antenna to the laboratory surrounding, a Faraday cage was built.

4.3 Antenna and antenna positioning

To create an electric field to proximity of laser induced plasma, a high power near field microwave antenna was used. Both, helical and tip antenna were tested but the tip antenna was chosen for further investigations due easier alignment. Both antennas performed somewhat equally when the enhancement was compared. The tip antenna was constructed from RG-402/U semi-rigid coaxial cable in which the core material was 0.93 mm thick silver plated copper steel which has extremely good microwave conduction properties. The earthed cladding was stripped off 30 mm distance from the tip of the cable and dielectric PTFE insulator is removed. This corresponds approximately the $\lambda/4$ distance, where λ is the wavelength of the microwave radiation. Tip of the antenna was polished and sharpened to approximately 45 degree angle. Microwave pulse was transported from the waveguide to the antenna with LMR-400 coaxial cable. LMR-400 has copper cladded aluminum core with thickness of 2.74 mm and therefore waveguide coupled well with it.

To investigate the electric field created by the antenna, a computer model was made. The model was constructed by using Comsol software. Finite element method (FEM) was applied to the problem because its ability to handle complicated geometries. The algorithm solves the Helmholtz equation for rotationally symmetric electric field in air and in dielectric media shown as a net area in Fig 4.3. The net is representing the density of the calculated data points. As a feed, a coaxial feed is used. At the artificially cut coaxial port, a port condition for electric field $E_0 + rE_0$ holds. In port condition equation, E_0 is the known TEM_{00} coaxial feed electric field

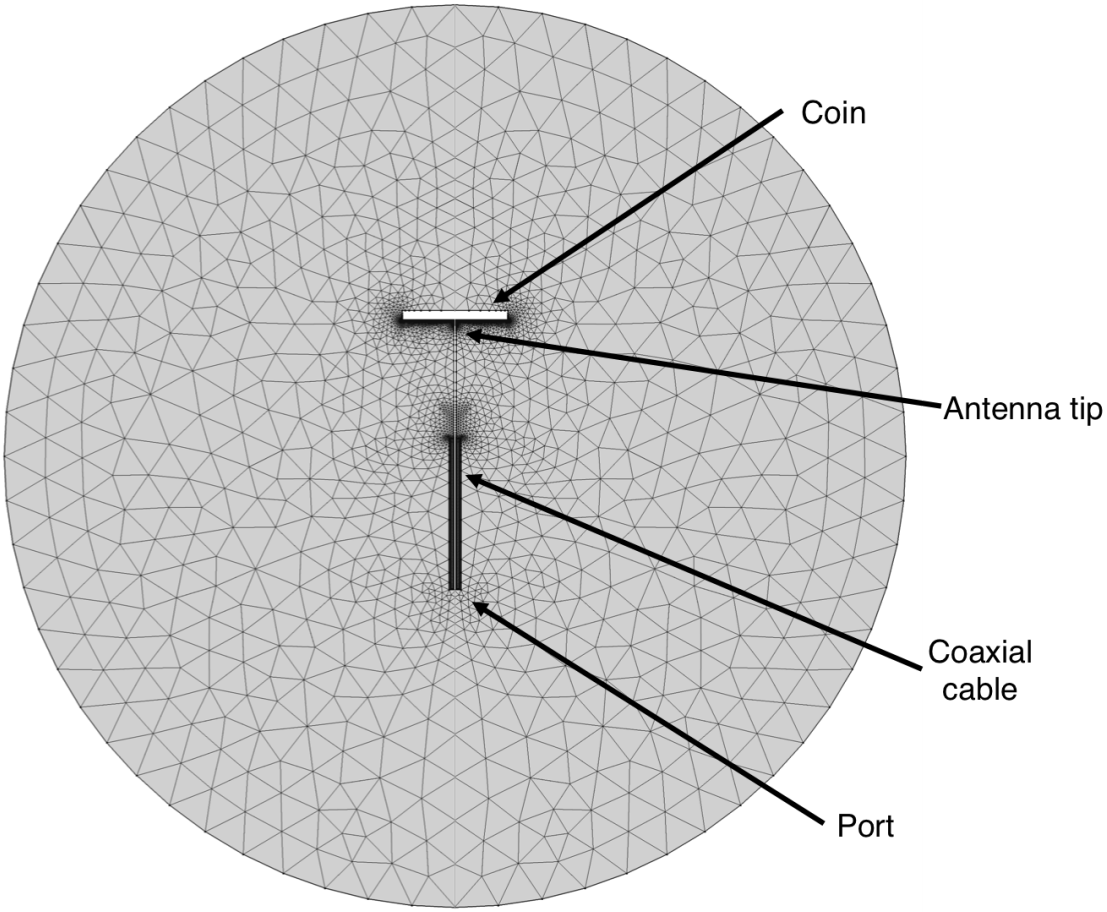

Figure 4.3 *The mesh used to model the electric field in the proximity of the antenna.*

and rE_0 is the reflected electric field as r is the unknown reflection coefficient. The input power is 1 W. As a sample in the model, a copper coin was placed 1 mm away from the tip to the longitudinal axis. The absolute value of calculated electric field in longitudinal direction along the antenna is plotted in Fig4.4(a). In Fig4.4(b) is shown the electric field in latitudinal direction at two different distances from the antenna tip. As seen in the Fig 4.4, the electric field attenuates quickly when moved further away from the antenna tip. Therefore antenna tip is positioned as close as possible to the sample without contaminating it.

Antenna was positioned close to the ablation spot to create strong electric field to the plasma as shown in Fig 4.5. Antenna was placed on a mount which allowed precise control of the antenna tip in all dimensions. No separate measurement chamber was set to surround the antenna but all measurements were performed in ambient

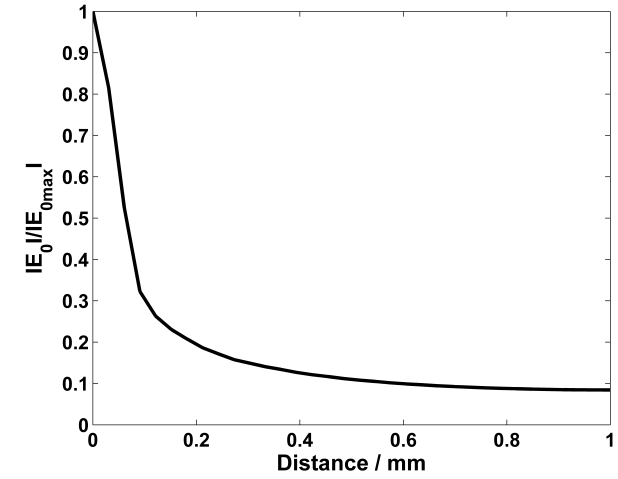

(a)

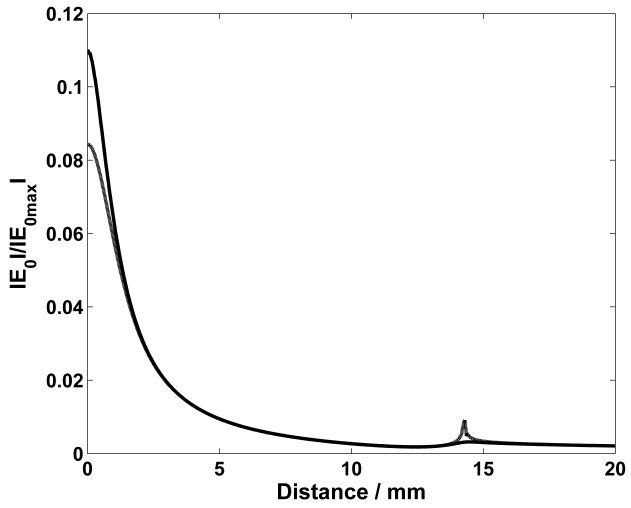

(b)

Figure 4.4 *The modeled normalized absolute value of electric field emitted from the tip antenna. a) The electric field in longitudinal direction along the antenna axis and b) electric field in latitudinal direction at two different longitudinal distance from the antenna tip. Solid line 0.5 mm away from the tip and dashed line 1mm away from the tip.*

air and pressure. As antenna material contained copper which was chosen to be the target element, a compromise between stable and effective plasma enhancement and avoiding the contamination of signal with the antenna tip had to be found. By observing the plasma and measuring a blank sample, a suitable position was found to be 0.5 mm horizontally away from the ablation spot and 1 mm above the sample.

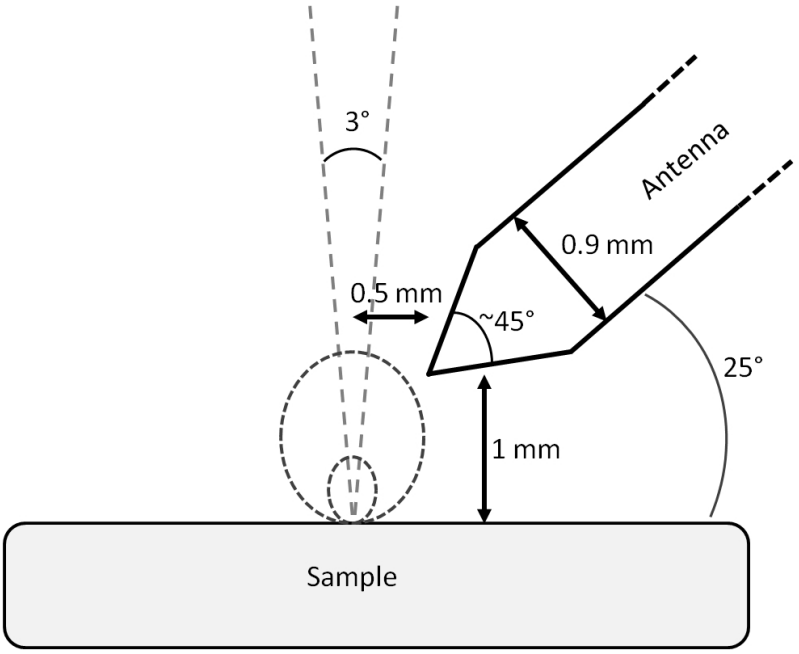

Figure 4.5 *Schematic illustration of the antenna positioning and measures. Smaller dashed circle represents the time averaged size of plasma induced by conventional LIBS and larger dashed line the plasma enhanced with microwave.*

As blank samples, copper free samples with similar sample matrix to actual samples was used. Samples and their production are described in section 4.5. Antenna was tilted to 25 degree angle tip pointing to the sample surface. This was done to avoid arching between the antenna and the sample.

4.4 Timing of pulses

To succeed in microwave enhancement, the timing between the microwave, laser and ICCD camera has to be well controlled. A delay generator (Princeton Instruments) was used to control the timing between the setup components. The microwave pulse is triggered at the same time as the laser flash lamp. This gives microwave source time to reach the maximum output power which it was adjusted to maintain for 2 ms. Microwave source would be able to produce even shorter pulses but the output and reflected microwave power meters were not able to follow shorter pulses. Short pulse width was required to avoid overheating the antenna. Delay between flash lamp and Q-switch was 180 μs which was enough for microwave pulse to reach its maximum value. ICCD was triggered 1 μs after the laser pulse. This was made to

avoid the intensive background radiation emitted from the plasma in the beginning of its formation. Timing between the components is illustrated in Fig 4.6.

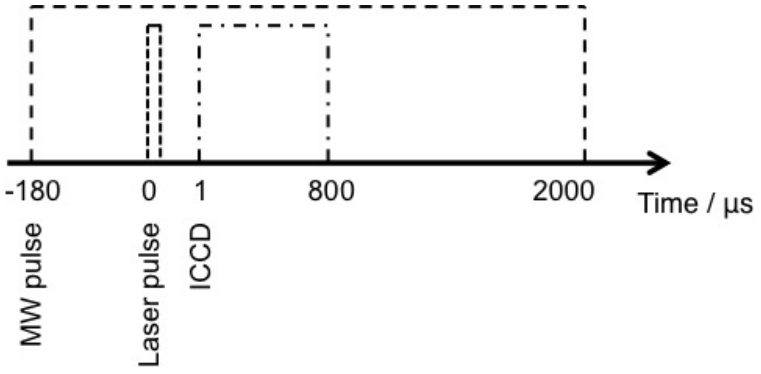

Figure 4.6 *Schematic graph of timing between the microwave pulse, laser pulse and ICCD*

4.5 Sample preparation

To investigate the optimal conditions for antenna coupled microwave enhanced LIBS, a sample with well known copper concentration and good availability was chosen. The sample used was Australian 20 cent coin having 75 w-% of copper. Sample was chosen because of homogeneous concentration and a relatively flat surface. Irregularities on the coin surface did not show any effect on averaged signals. As an blank sample for coin, metallic aluminum was used.

For being able to measure accurate calibration curves for both conventional and microwave enhanced LIBS, calibration samples with known copper concentration were required. Wet impregnation was used to produce copper catalysts with 0.2 w-%, 0.4 w-%, 0.7 w-% and 0.12 w-% of copper. Al_2O_3 was used as a catalyst support and to dilute the catalysts to achieve even lower copper concentrations. At first, the catalyst support and the source of wanted catalyst material were accurately weighted out. $Cu(NO_3)_2{\cdot}3H_2O$ was used as a source of copper. Weighted aluminum oxide and copper nitrite were diluted to deionized water and placed in to a beaker where they were baked and stirred well while their pH was adjusted to 10 with NaOH. The resulting solutions were then distilled and dried in oven. Dried solution was then oxidized for 6 hours in 850 °C muffle furnace. Resulting catalyst was fine powder containing the wanted concentration of copper. For LIBS analysis, powder

was placed into a plastic mold and mixed with a hint of spray adhesive to avoid pit formation to the sample when exposed to the laser radiation. The surface of the sample was smoothen by compression. Blank sample for low concentration copper samples was produced similarly to actual samples from pure Al_2O_3.

Mineral samples used for examining the applicability of microwave enhancement were obtained from an Australian mine in New South Wales. Mineral samples were cut and the cut surface was polished for smooth measurement surface. This enabled keeping the lens to sample distance constant, and more homogeneous ablation conditions reduced the signal variation rising from the ablation process.

To minimize the signal variation due sample matrix, the sample was placed on moving mount which rotated and made linear transition. This enabled scanning of whole sample area. The sample movement also caused each laser shot to hit new spot on the sample surface and therefore the homogeneity of the ablation conditions were even further improved.

5. RESULTS AND DISCUSSION

Antenna coupled microwave enhancement of conventional LIBS was studied by measuring the intensity of atomic copper (Cu I) transition $4s^2S_{1/2}$-$4p^2P^0{}_{1/2}$ which emits an emission line at 324.75 nm. Optimal measurement parameters: gate width, gate delay, laser pulse energy and microwave power were determined by using Australian 20 cent coin containing copper as a target.The intensity of the emission was gained by measuring 100 shots from a moving sample, averaging them and integrating the counts over the line profile. Intensities obtained by conventional LIBS and microwave enhanced LIBS were compared and their behavior was studied. All measurements were done at atmospheric pressure in the ambient air. The results of these experiments are presented in this chapter and their meaning is discussed.

5.1 Temporal evolution of fluorescent signal

The temporal evolution of laser induced plasma was studied by measuring short temporal window with ICCD camera and delaying the measurement with short increments. Laser pulse energy was set to 2.5 mJ. For conventional LIBS measurement gate width of 2 μs was used and the signal acquisition was delayed from 0 to 12 μs. As shown in Fig5.1(b), the intensity of Cu I emission line at 324.75 nm was observed to decay exponentially below the noise level in 15 μs and the signal could not be detected with longer delay times. Short decay time of the emission intensity forces short acquisition times to be used. This is one of the limiting factors for the LIBS sensitivity. From the information obtained, for further conventional LIBS measurements the gate width was decided to be 10 μs with 1 μs delay from the laser pulse.

When microwave radiation was applied to the laser induced plasma, a substantial extension of plasma lifetime was observed. The measurement gate width for microwave enhanced plasma was 100 μs and the delay was from 0 to 2000 μs. Intensity of the copper line in interest decayed in double exponential manner. The first phase

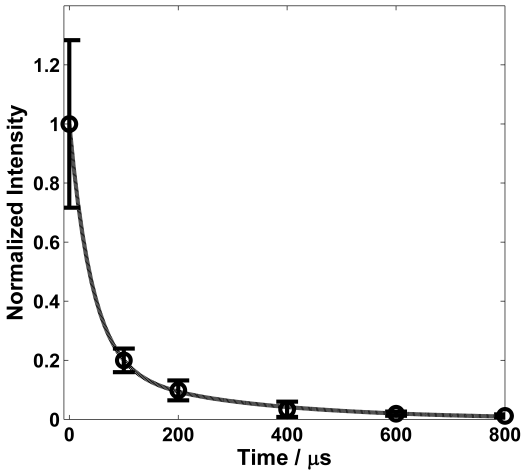

(a)

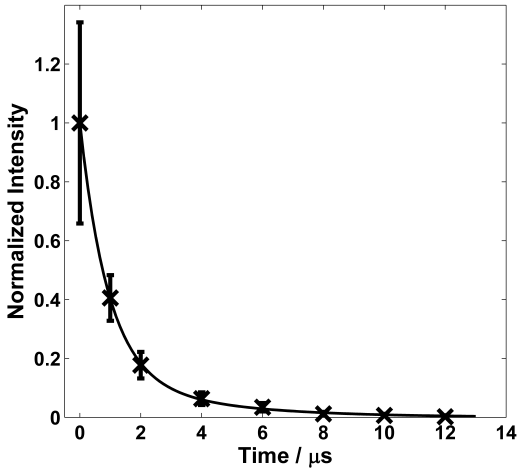

(b)

Figure 5.1 *Normalized intensity of Cu I 324.75 μm line as a function of time. a) MW on, MW power 1.2 kW, b) MW off.*

was fast decay with similar trend than conventional LIBS. The second phase of the decay was much slower due the presence of the microwave induced electric field. Electric field starts to affect to the plasma decay as the electron density decays under the critical level. This is when the plasma shield becomes transparent for the microwave. The emission remains on detectable level as long as the 2 ms long microwave pulse is applied to the laser induced plasma. As seen in Fig5.1(a), most

of the signal lies within the first 800 μs and therefore it was decided that for further investigations the gate width of 800 μs would be used. It was also noticed that the continuous background radiation from the early state of the plasma decays to ignorable level in 1 μs and therefore a delay of 1 μs was decided to use in further experiments. The error bars in Fig 5.1 is the standard deviation of 100 single shot signals. The larger deviation in microwave enhanced case is due the increased complexity of the signal formation. As the initial laser induced plasma varies from shot to shot, so does the coupling between the microwave radiation and plasma.

To examine the effect of microwave to the early evolution of the laser induced plasma, similar measurement was performed as described above but using 500 ns long gate width and the signal acquisition was delayed from 0 to 5 μs. To emphasize the difference between microwave enhanced LIBS and conventional LIBS, laser pulse energy of 0.8 mJ was used. As can be seen in Fig 5.2, the first μs of the plasma lifetime is very similar in the microwave enhanced case and in conventional laser induced plasma. The initial signal level is on same level and decay rate is the same during first 2 μs. After 2 μs the electron density has decreased under the critical level 7×10^{10} cm^{-3} for microwave radiation used. This is when the the microwave radiation begins to re-heat the plasma plume. As the radiation can propagate through the plasma, it starts to re-heat the plasma and therefore maintain the signal level as can be seen in Fig5.2(a) This kind of re-heating of low-density plasma is very useful since it does not re-heat the plasma continuum which occur in the most intensive state of plasma, but neglects it and improves therefore the signal to noise ratio significantly which eventually leads to improved limit of detection.

5.2 Effect of microwave power and laser pulse energy

Effect of microwave source power was studied by setting laser pulse energy to 2.5 mJ and varying the microwave source power from 0 to 2 kW. Microwave source output power was set with the pulse generator and measured with source's internal power meter. In region 1 in Fig 5.3, the coupling efficiency to the antenna was approximately 70 % which was measured by following the back reflected microwave power. As the source power was increased over 1.2 kW the coupling efficiency was noted to change. In region 2, the average coupling efficiency decreased and its shot to shot variation was significant. This might be due the lack of coaxial cable ability to intake and carry power. Reliable analysis of the effect of microwave power could therefore be conducted only in region 1. Inside region 1, the intensity of the copper

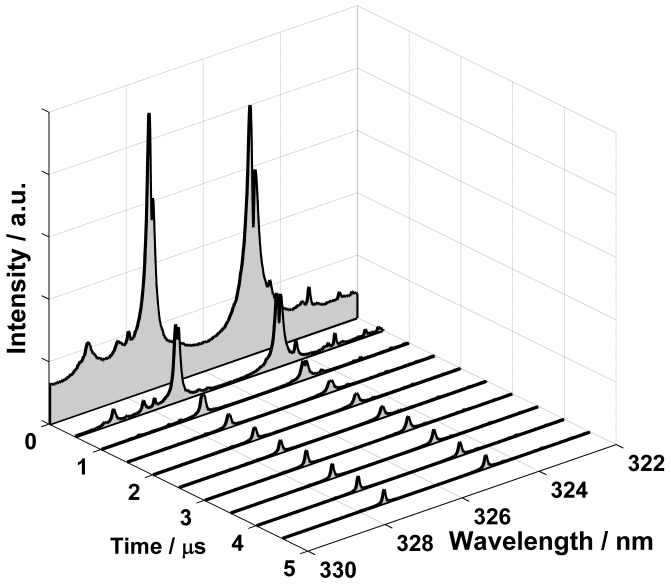

(a)

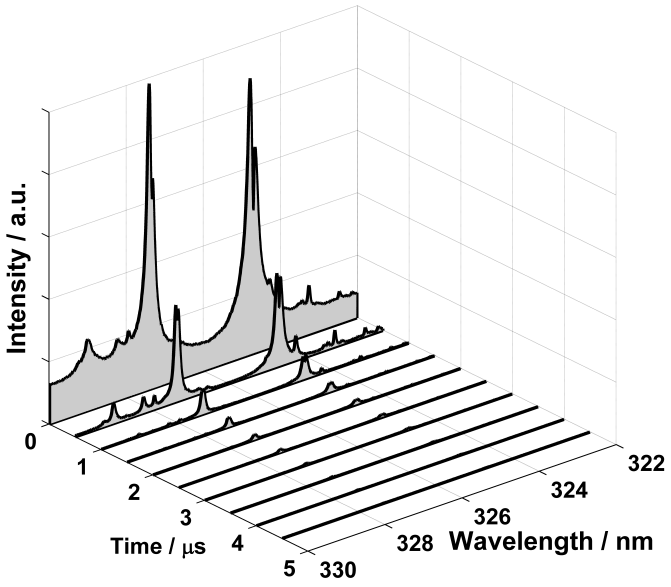

(b)

Figure 5.2 *High resolution spectra of early evolution of the laser induced plasma as a function of time. a) MW on, MW power 1.2 kW, b) MW off.*

line exhibited exponential increase as the microwave source power was increased. For further experiments microwave source power was decided to be fixed to 1.2 kW which was the maximum source power able to maintain the 70 % coupling efficiency.

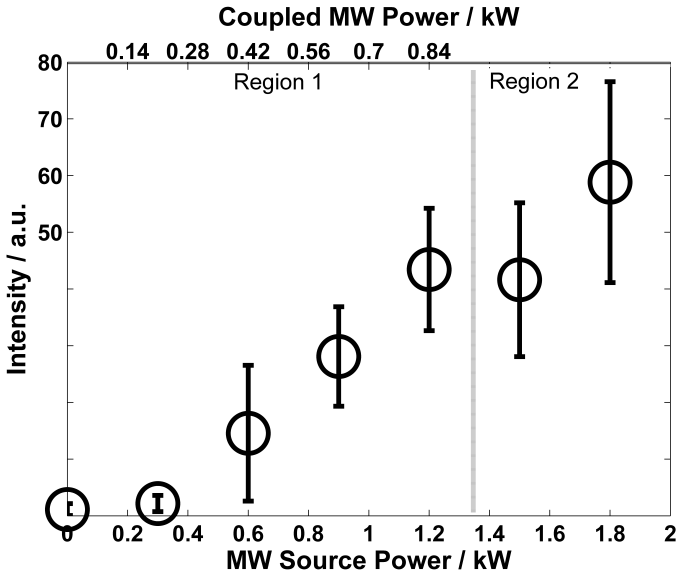

Figure 5.3 *Intensity of Cu I 324.75 nm line as a function of microwave power. In region 1 the coupling efficiency of microwave stays constant at 70 % but when moved to region 2 the coupling efficiency decreases.*

To examine the effect of change in the laser pulse energy, microwave power was kept constant and laser pulse energy was varied from 0.5 to 15 mJ. Energy of the laser pulse was tuned by rotating the half-wave plate and the energy was measured with a power meter. As can be seen in Fig 5.4, the intensity of the copper line exhibits peculiar behavior around 2 mJ energy when microwave radiation was applied to laser induced plasma. Instead of linear trend, which conventional LIBS typically represents, a bump is observed. With laser pulse energies of 2 to 2.5 mJ similar signal intensity to energies of 7 mJ was measured. The behavior can be explained by assuming that at the 2 mJ energy, the size of laser induced plasma matches well to the size of intensive electric field produced by the antenna and the overall plasma size matches with the signal collection. Larger plasma cannot be maintained as effectively by the microwave and the maintained part is not at optimal position for the signal collection. Therefore the signal actually remains the same or even slightly decreases as the laser pulse power is increased over 2.5 mJ. For higher energies than

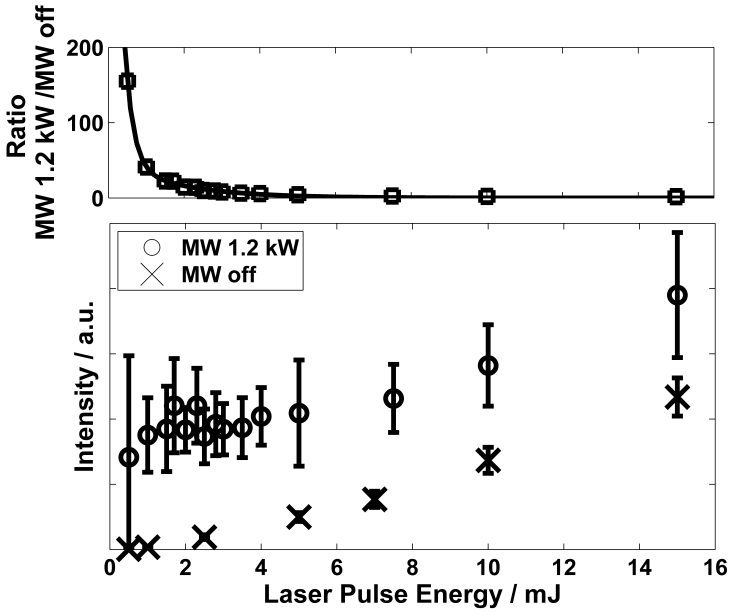

Figure 5.4 *Intensity of Cu I 324.75 nm line as a function of laser pulse energy and above is the calculated ratio of MW on and MW off cases.*

7 mJ also microwave enhanced LIBS signal starts to follow linear trend. To achieve the best signal and get maximum advantage from the microwave system, the laser pulse energy for further measurements was set to 2.5 mJ. 2.5 mJ was chosen to produce stable coupling between the electric field produced by the antenna and the laser induced plasma.

The calculated ratio of MW enhanced LIBS signal and conventional LIBS signal in Fig 5.4 shows that the maximal enhancement is achieved with low laser pulse energies. Large error bar in the low laser pulse energy measurement is due the instability of the initial laser induced plasma. It was noted that 0.5 mJ laser pulse energy was very close to the ablation threshold of the sample. But as the plasma was ignited the microwave was able to interact with it and good signal levels were observed. From the ratio, one can also see that conventional LIBS would eventually reach the signal level of microwave enhanced LIBS if laser pulse energy would be increased. At 15 mJ pulse energy the intensity ratio is 1.6.

5.3 Microwave effect on line profile

As the copper transition in interest is a ground state transition, it is very prone for self-absorption. And indeed, the self-absorption is clearly visible in the line profile measured with conventional LIBS in Fig5.5(a) and in Fig5.6(a). The tip of the peak is strongly self-reversed and the effect is visible even in very low laser pulse energies. When the conventional LIBS line profile is compared with the profile measured with presence of microwave radiation a difference is observed. The microwave enhanced line profile is not turned inside as seen in Fig5.5(b) and in Fig5.6(b). The improvement of line shape might be due the fact that a large part of the signal collected with microwave enhancement is from a temporal window when electron density has decreased. With lower electron density, plasma is not as optically thick as in the very beginning of plasma evolution where electron and atomic density is significantly higher. Practically all signal collected with conventional LIBS is from the plasma state at which plasma is optically thick and therefore self-absorption in high concentration samples cannot be avoided. Whereas microwave enhancement prolongs the plasma lifetime, and especially lifetime of the plasma state with lower electron density and therefore optically less dense. This effect improves the analytical performance in the case of high concentration samples as the self-absorption does not disturb the interpretation of the measurement results.

5.4 Analytical performance

To investigate the analytical performance with low laser pulse energy of antenna-coupled microwave enhancement, a calibration curve of Cu I line at 324.75 nm was measured with the low copper concentration samples produced. To compare the obtained curve, a calibration curve for conventional LIBS was also measured. The curves are plotted in Fig 5.7. Laser pulse energy was set on 2.5 mJ and microwave source power on 1.2 kW. Measured intensities exhibited linear behavior as expected and linear regression fits were fitted to the measured data. The slopes of fitted curves are 2277 and 20.2 for microwave enhanced LIBS and conventional LIBS respectively. The ratio of the microwave enhanced LIBS and conventional LIBS fitted slopes is 112.7 which already implies much better sensitivity for microwave enhanced LIBS. Microwave enhanced LIBS also represents better linearity than conventional LIBS with R^2 being 0.993 against R^2 for conventional LIBS being 0.917. Linearity and slope of signals from low concentration samples also shows that the positioning

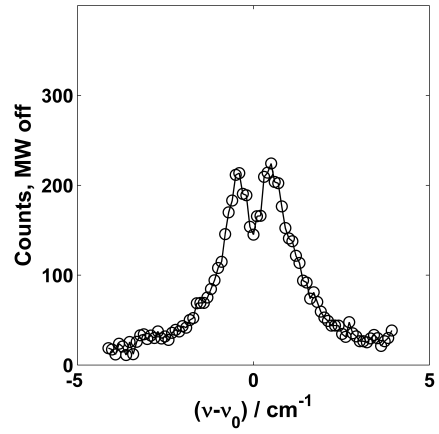

(a)

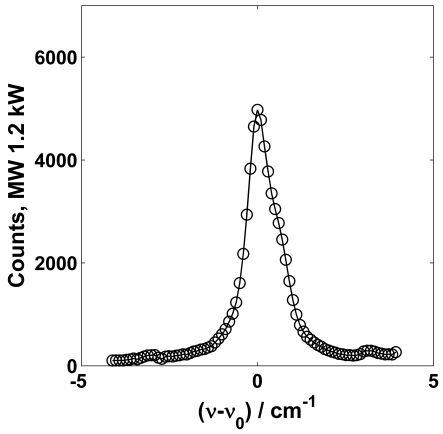

(b)

Figure 5.5 *Cu I 324.75 nm line profile with 2.5 mJ laser pulse energy. a) Microwave off, b) microwave 1.2 kW*

of antenna has been successful and the copper contained by the antenna has not disturbed the measurement. As copper concentration of the samples were significantly lower than the concentration in the antenna, in the case of contamination, the changes of concentartion in the samples would not have been detectable.

The limit of detection for each method can be calculated by applying the slope of the

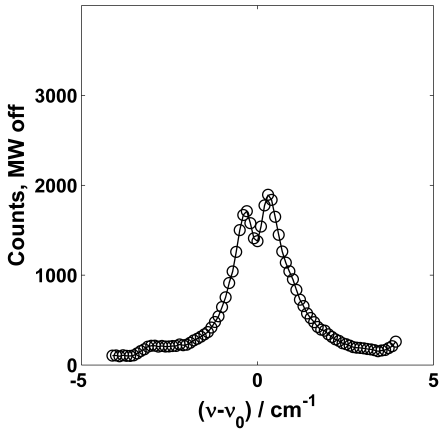

(a)

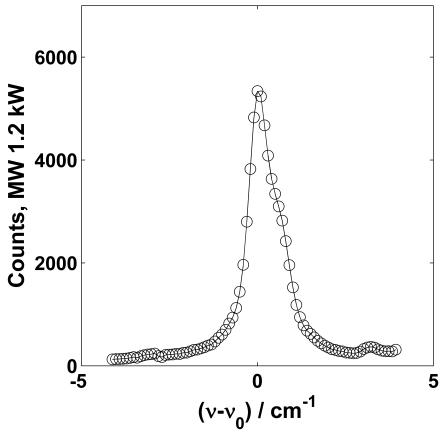

(b)

Figure 5.6 *Cu I 324.75 nm line profile with 10 mJ laser pulse energy. a) Microwave off, b) microwave 1.2 kW*

fitted calibration curve as shown in Equation 2.29. For conventional LIBS, calculated limit of detection for Cu I 324.75 nm line is 754 ppm. The high limit of detection was expected for low laser pulse energy. For microwave enhanced LIBS limit of detection is 8.1 ppm. This is 93 fold improvement compared to conventional LIBS at low laser pulse energy and compares well to the lowest detection limits achieved

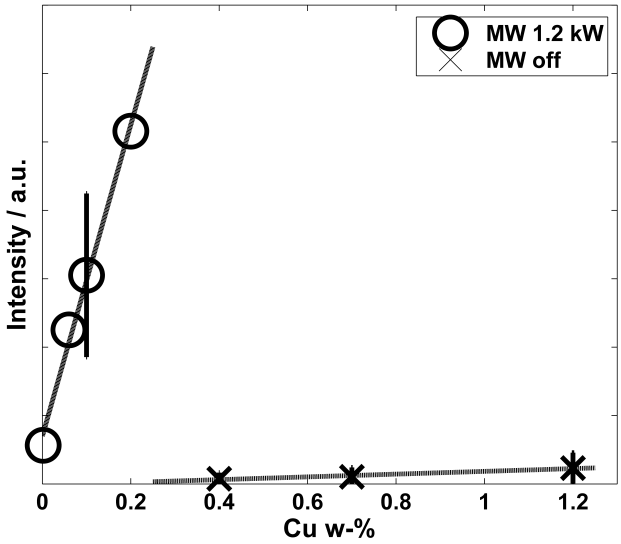

Figure 5.7 *Calibration curve for Cu I 324.75 nm line.*

with conventional LIBS using extremely high laser pulse energies. [32] These results shows the greatest benefits that can be gained with antenna-coupled microwave enhancement. With relatively simple and inexpensive addition to conventional LIBS setup, the analytical performance can be improved significantly. Low laser pulse energies can be used without compromising the sensitivity which enables the use of smaller low energy lasers and less damage is caused to the sample.

The intensive emission signal from microwave enhanced plasma enables also other interesting features to improve LIBS analysis. High resolution measurements require more intensive light input to the detector. For example, detection of Uranium (U) requires extremely high resolution spectrometers due its large number of emission lines. [67] Also separation of isotopes require high resolution due the proximity of emission lines of different isotopes. [68] Plasma enhancement with microwave could help with these tasks. High intensities of plasma emitted radiation enable also use of cheaper CCD detectors instead of ICCD detectors. Typically CCD detectors have too long signal integration time for conventional LIBS which decreases the signal to noise ratio but, as the signal of microwave enhanced LIBS is longer, CCD detector could work well with the microwave enhanced plasmas. In the case of most intensive separate emission lines, spectrometer could be replaced with filters and simple photodetector to detect a single elemental line.

5.5 Application to mineral samples

Antenna-coupled microwave enhanced LIBS was applied on a mineral sample collected from a mine in New South Wales in Australia. Low resolution spectra from 300 nm to 475 nm was measured with and with out microwave enhancement. Obtained spectra are presented in Fig 5.8. From measured spectra, it was observed that the enhancement affects to all emission lines but not necessarily in the same ratios. It seems that the enhancement is more efficient in the shorter wavelengths than in the longer wavelengths. This could be explained with higher electron temperature induced by the electric field when the population in the upper energy levels becomes larger and makes high upper level transitions transitions more probable. The observation, that the enhancement has an effect to all elements is important as it shows that the enhancement effect for copper lines is not due contamination from the antenna and expresses the versatility of the technique.

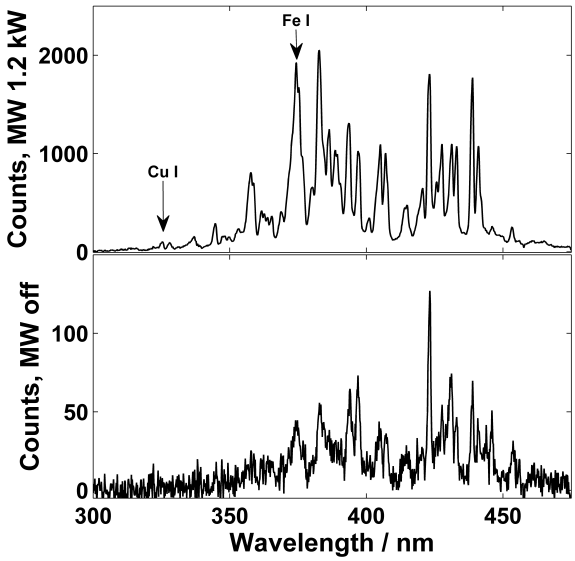

Figure 5.8 *Typical microwave enhanced LIBS spectra and traditional LIBS spectra with low resolution measured from a mineral sample.*

When high resolution spectra in Fig 5.9 are compared, the advantage of microwave enhancement becomes very clear. Conventional LIBS cannot measure the copper concentration in the mineral sample with the low laser pulse energy but antenna-coupled microwave enhanced LIBS presents clear copper lines. It even shows Cu I

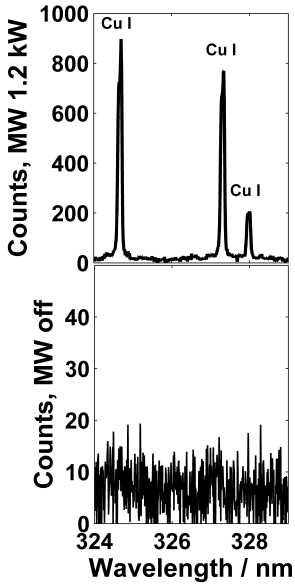

Figure 5.9 *Typical microwave enhanced LIBS spectra and traditional LIBS spectra with high resolution measured from a mineral sample.*

emission line at 328 nm which is not a ground state transition and requires electron population to higher energy levels. This observation also implies that higher electron temperature is achieved with the microwave enhanced LIBS.

Antenna-coupled microwave enhanced LIBS shows good potential for mineral analysis and could be good option to reduce price of LIBS device while improving the analytical performance. So far the main problem with antenna-coupled microwave enhanced LIBS is that it does not work well on the raw mineral surface but requires some sample preparation to get smooth measurement surface. Measurement on rough surface is tricky as the antenna to sample distance, and therefore also the antenna to plasma distance, varies and this causes variation to the coupling between plasma and the electric field. This is seen as unstable signal. On the other hand, when low laser pulse energies are used, sample does not necessarily need to be moved after every laser shot. Still it would be challenging to position the antenna on the surface so that a reliable signal and a stable microwave coupling to plasma are achieved. But even if it would be required to manually choose or cut a rock for the measurement, the sample preparation is reduced compared to other microwave enhancement techniques discussed in Chapter 3. Current method

also enables measurement to be performed in the ambient air and pressure which decreases the requirements for the measurement environment. No separate measurement cavity nor chamber is required to cover the sample which speeds up the measurement procedure. This significantly simplifies it and makes antenna-coupled microwave enhancement an attractive option to improve analytical performance of online analysis of different industrial products. Ability to work with laser energies near the ablation threshold is advantage when only a small amount of sample is available or no damage is wanted to cause. This is the case in, for example, analysis of art work and in forensic applications.

6. CONCLUSIONS

Elemental detection on solid objects is an issue on multiple fields of industry and science. Laser induced breakdown spectroscopy (LIBS) has been proven to be excellent candidate for this task. The main obstacles for LIBS to become the standard in elemental analysis are the difficulties in quantitative analysis and the lack of sensitivity. In this thesis antenna-coupled microwave radiation is applied to improve the sensitivity of LIBS measurement on solid samples at atmospheric pressure. A near field tip antenna was used to radiate microwave radiation to the laser induced plasma. Compared to conventional LIBS, almost 100 fold improvement to the sensitivity and to the limit of detection was achieved. The improvement of the acquired signal is mainly due the prolonged lifetime of laser induced plasma. Through the re-heating effect, the plasma lifetime can be prolonged to ms timescale. The microwave maintained plasma is optically thin compared to conventional laser induced plasma. This is observed to decrease the self-reversing effect, which is beneficial in high concentration measurements.

As an enhancement method, antenna-coupled microwave enhancement stands well in the comparison with other enhancement methods. Table 6.1 shows the figures of merit of different enhancement methods. Among microwave enhancement methods, the antenna-coupled microwave enhancement performed in this thesis resembles the best potential for LIBS enhancement. Current study also overcame the issue with atmospheric pressure, which has been earlier the limiting factor for antenna-coupled microwave enhanced LIBS applications. This is an important factor when the applicability of the technique is considered.

In addition to its potential to significantly increase the sensitivity of LIBS measurement, antenna-coupled microwave enhancement is simple, easy to use and inexpensive enhancement method. The main requirement for the measurement sample is

Table 6.1 *Summary of the best enhancement factors achieved with different LIBS enhancement methods*

Element	Sample	Method	Enhancement factor	LOD (ppm)	Reference
Cr I	Metal alloy	Spatial confinement	24		[48]
Al I	Metal alloy	DP-LIBS	80		[53]
Cu I	Metal alloy	DP-LIBS	30		[53]
Fe I	Ceramic	CO_2 DP-LIBS	119		[54]
Al II	Metal alloy	SD-LIBS	50-400		[56]
Al I	Metal alloy	Flame assisted	4		[58]
Na I	Ceramic	Enclosed MW cavity	33		[60]
Cu I	Soil	Enclosed MW cavity	23	30	[63]
Gd II	Gd_2O_3	Loop MW antenna	32	2	[65]
Gd II	Gd_2O_3	Loop MW antenna	50		[66]
Cu I	Cu/Al_2O_3	Tip MW antenna	93	8.1	This work

that it possess somewhat smooth surface on which the antenna tip can be accurately positioned. This only, easily delivered, requirement makes antenna-coupled microwave enhanced LIBS an interesting possibility to improve elemental detection in various targets and disciplines. Next steps in the development of antenna-coupled microwave enhanced LIBS would be to stabilize the microwave-plasma coupling by studying the antenna positioning and antenna geometry further. By careful antenna design, larger part of the energy carried by the microwave radiation could be deposited to the laser induced plasma. This would decrease the power requirements for the microwave source and therefore decrease also the price and need of external devices, such as water cooling. On the other hand, high power microwave obviates the high laser pulse energy to gain good sensitivity and high signal levels. This could open a possibility to use fiber coupled laser system, which would further improve the applicability of LIBS analysis to industrial needs.

BIBLIOGRAPHY

[1] D. A. Cremers and L. J. Radziemski, *Handbook of Laser-Induced Breakdown Spectroscopy*. John Wiley & Sons, Ltd, 2006.

[2] D. W. Hahn and N. Omenetto, "Laser-induced breakdown spectroscopy (LIBS), part i: Review of basic diagnostics and plasma–particle interactions: Still-challenging issues within the analytical plasma community," *Appl. Spectrosc.*, vol. 64, no. 12, pp. 335A–366A, Dec 2010.

[3] ——, "Laser-induced breakdown spectroscopy (LIBS), part ii: Review of instrumental and methodological approaches to material analysis and applications to different fields," *Appl. Spectrosc.*, vol. 66, no. 4, pp. 347–419, Apr 2012.

[4] S. T. Järvinen, S. Saari, J. Keskinen, and J. Toivonen, "Detection of Ni, Pb and Zn in water using electrodynamic single-particle levitation and laser-induced breakdown spectroscopy," *Spectrochimica Acta Part B: Atomic Spectroscopy*, vol. 99, pp. 9–14, 2014.

[5] M. Guilhaus, D. Selby, and V. Mlynski, "Orthogonal acceleration time-of-flight mass spectrometry," *Mass Spectrometry Reviews*, vol. 19, no. 2, pp. 65–107, 2000.

[6] M. F. Bean, S. A. Carr, G. C. Thorne, M. H. Reilly, and S. J. Gaskell, "Tandem mass spectrometry of peptides using hybrid and four-sector instruments: A comparative study," *Analytical Chemistry*, vol. 63, no. 14, pp. 1473–1481, 1991, pMID: 1718187.

[7] R. A. Yost and C. G. Enke, "Triple quadrupole mass spectrometry for direct mixture analysis and structure elucidation," *Analytical Chemistry*, vol. 51, no. 12, pp. 1251–1264, 1979, pMID: 21902234.

[8] P. S. Wong and R. Graham Cooks, "Ion trap mass spectrometry," *Current separations*, vol. 16, pp. 85–92, 1997.

[9] G. Jenner, H. Longerich, S. Jackson, and B. Fryer, "ICP-MS a powerful tool for high-precision trace-element analysis in earth sciences: evidence from analysis of selected USGS reference samples," *Chemical Geology*, vol. 83, no. 1, pp. 133–148, 1990.

[10] X. Li, B. J. Coles, M. H. Ramsey, and I. Thornton, "Sequential extraction of soils for multielement analysis by ICP-AES," *Chemical Geology*, vol. 124, no. 1, pp. 109–123, 1995.

[11] B. Magyar and F. Aeschbach, "Why not icp as atom reservoir for AAS?" *Spectrochimica Acta Part B: Atomic Spectroscopy*, vol. 35, no. 11, pp. 839–848, 1980.

[12] Y. Liu, Z. Hu, S. Gao, D. Günther, J. Xu, C. Gao, and H. Chen, "In situ analysis of major and trace elements of anhydrous minerals by LA-ICP-MS without applying an internal standard," *Chemical Geology*, vol. 257, no. 1, pp. 34–43, 2008.

[13] M. Hollas, J. Michael, *Modern spectroscopy.* John Wiley & Sons, 2004.

[14] S. Ray and A. G. Shard, "Quantitative analysis of adsorbed proteins by X-ray photoelectron spectroscopy," *Analytical chemistry*, vol. 83, no. 22, pp. 8659–8666, 2011.

[15] D. M. Hercules, L. E. Cox, S. Onisick, G. D. Nichols, and J. C. Carver, "Electron spectroscopy (ESCA). use for trace analysis," *Analytical Chemistry*, vol. 45, no. 11, pp. 1973–1975, 1973.

[16] J. Hanawalt, H. Rinn, and L. Frevel, "Chemical analysis by X-ray diffraction," *Industrial & Engineering Chemistry Analytical Edition*, vol. 10, no. 9, pp. 457–512, 1938.

[17] V. Guinn and J. Hoste, "Neutron activation analysis," *Elemental Analysis of Biological Materials*, pp. 105–140, 1980.

[18] D. L. C. Savio, M. A. Mariscotti, and S. R. Guevara, "Elemental analysis of a concrete sample by capture gamma rays with a radioisotope neutron source," *Nuclear Instruments and Methods in Physics Research Section B: Beam Interactions with Materials and Atoms*, vol. 95, no. 3, pp. 379–388, 1995.

[19] R. Gower and I. Rhodes, "A review of techniques in the Lassaigne sodium-fusion," *Journal of Chemical Education*, vol. 46, no. 9, p. 606, 1969.

[20] D. Ayres and B. Dawson, "Use of the oxygen flask in organic qualitative analysis," *Journal of Chemical Education*, vol. 42, no. 5, p. 270, 1965.

[21] C. Lopez-Moreno, S. Palanco, J. J. Laserna, F. DeLucia Jr, A. W. Miziolek, J. Rose, R. A. Walters, and A. I. Whitehouse, "Test of a stand-off laser-induced breakdown spectroscopy sensor for the detection of explosive residues on solid surfaces," *Journal of Analytical Atomic Spectrometry*, vol. 21, no. 1, pp. 55–60, 2006.

[22] B. Sallé, J.-L. Lacour, E. Vors, P. Fichet, S. Maurice, D. A. Cremers, and R. C. Wiens, "Laser-induced breakdown spectroscopy for Mars surface analysis: capabilities at stand-off distances and detection of chlorine and sulfur elements," *Spectrochimica Acta Part B: Atomic Spectroscopy*, vol. 59, no. 9, pp. 1413–1422, 2004.

[23] A. K. Knight, N. L. Scherbarth, D. A. Cremers, and M. J. Ferris, "Characterization of laser-induced breakdown spectroscopy (LIBS) for application to space exploration," *Applied Spectroscopy*, vol. 54, no. 3, pp. 331–340, 2000.

[24] G. Arca, A. Ciucci, V. Palleschi, S. Rastelli, and E. Tognoni, "Trace element analysis in water by the laser-induced breakdown spectroscopy technique," *Applied Spectroscopy*, vol. 51, no. 8, pp. 1102–1105, 1997.

[25] A. De Giacomo, M. DellAglio, and O. De Pascale, "Single pulse-laser induced breakdown spectroscopy in aqueous solution," *Applied Physics A*, vol. 79, no. 4-6, pp. 1035–1038, 2004.

[26] J.-S. Huang, C.-B. Ke, L.-S. Huang, and K.-C. Lin, "The correlation between ion production and emission intensity in the laser-induced breakdown spectroscopy of liquid droplets," *Spectrochimica Acta Part B: Atomic Spectroscopy*, vol. 57, no. 1, pp. 35–48, 2002.

[27] M. Tran, B. W. Smith, D. W. Hahn, and J. D. Winefordner, "Detection of gaseous and particulate fluorides by laser-induced breakdown spectroscopy," *Applied Spectroscopy*, vol. 55, no. 11, pp. 1455–1461, 2001.

[28] D. Hahn, "Laser-induced breakdown spectroscopy for sizing and elemental analysis of discrete aerosol particles," *Applied Physics Letters*, vol. 72, no. 23, pp. 2960–2962, 1998.

[29] D. Hahn and M. Lunden, "Detection and analysis of aerosol particles by laser-induced breakdown spectroscopy," *Aerosol Science & Technology*, vol. 33, no. 1-2, pp. 30–48, 2000.

[30] A. Ciucci, M. Corsi, V. Palleschi, S. Rastelli, A. Salvetti, and E. Tognoni, "New procedure for quantitative elemental analysis by laser-induced plasma spectroscopy," *Applied spectroscopy*, vol. 53, no. 8, pp. 960–964, 1999.

[31] I. Rauschenbach, V. Lazic, S. Pavlov, H.-W. Hübers, and E. Jessberger, "Laser induced breakdown spectroscopy on soils and rocks: Influence of the sample temperature, moisture and roughness," *Spectrochimica Acta Part B: Atomic Spectroscopy*, vol. 63, no. 10, pp. 1205–1215, 2008.

[32] W. T. Y. Mohamed, "Improved LIBS limit of detection of Be, Mg, Si, Mn, Fe and Cu in aluminum alloy samples using a portable echelle spectrometer with ICCD camera," *Optics & Laser Technology*, vol. 40, no. 1, pp. 30–38, 2008.

[33] E. Hecht, *Optics*, 4th ed. Addison-Wesley, 1998.

[34] B. N. Chichkov, C. Momma, S. Nolte, F. von Alvensleben, and A. Tünnermann, "Femtosecond, picosecond and nanosecond laser ablation of solids." *Applied Physics A: Materials Science & Processing*, vol. 63, no. 2, p. 109, 1996.

[35] X. Liu, D. Du, and G. Mourou, "Laser ablation and micromachining with ultrashort laser pulses," *Quantum Electronics, IEEE Journal of*, vol. 33, no. 10, pp. 1706–1716, Oct 1997.

[36] J. Jacob, L. Chia, and F. Boey, "Thermal and non-thermal interaction of microwave radiation with materials," *Journal of Materials Science*, vol. 30, no. 21, pp. 5321–5327, 1995.

[37] W. Destler, J. DeGrange, H. Fleischmann, J. Rodgers, and Z. Segalov, "Experimental studies of high-power microwave reflection, transmission, and absorption from a plasma-covered plane conducting boundary," *Journal of applied physics*, vol. 69, no. 9, pp. 6313–6318, 1991.

[38] M. Boulos, P. Fauchais, and E. Pfender, *Thermal Plasmas*. Springer US, 1994.

[39] L. Cabalin and J. Laserna, "Experimental determination of laser induced breakdown thresholds of metals under nanosecond Q-switched laser operation," *Spectrochimica Acta Part B: Atomic Spectroscopy*, vol. 53, no. 5, pp. 723 – 730, 1998.

[40] M. Capitelli, A. Casavola, G. Colonna, and A. D. Giacomo, "Laser-induced plasma expansion: theoretical and experimental aspects," *Spectrochimica Acta Part B: Atomic Spectroscopy*, vol. 59, no. 3, pp. 271 – 289, 2004.

[41] N. Arnold, J. Gruber, and J. Heitz, "Spherical expansion of the vapor plume into ambient gas: an analytical model," *Applied Physics A*, vol. 69, no. 1, pp. S87–S93, 1999.

[42] R. Noll, *Laser Induced Breakdown Spectroscopy.* Springer-Verlag Berlin Heidelberg, 2012.

[43] A. M. Popov, F. Colao, and R. Fantoni, "Enhancement of LIBS signal by spatially confining the laser-induced plasma," *J. Anal. At. Spectrom.*, vol. 24, pp. 602–604, 2009.

[44] ——, "Spatial confinement of laser-induced plasma to enhance LIBS sensitivity for trace elements determination in soils," *J. Anal. At. Spectrom.*, vol. 25, pp. 837–848, 2010.

[45] L. B. Guo, C. M. Li, W. Hu, Y. S. Zhou, B. Y. Zhang, Z. X. Cai, X. Y. Zeng, and Y. F. Lu, "Plasma confinement by hemispherical cavity in laser-induced breakdown spectroscopy," *Applied Physics Letters*, vol. 98, no. 13, pp. –, 2011.

[46] L. Guo, Z. Hao, M. Shen, W. Xiong, X. He, Z. Xie, M. Gao, X. Li, X. Zeng, and Y. Lu, "Accuracy improvement of quantitative analysis by spatial confinement in laser-induced breakdown spectroscopy," *Opt. Express*, vol. 21, no. 15, pp. 18 188–18 195, Jul 2013.

[47] X. K. Shen, Y. F. Lu, T. Gebre, H. Ling, and Y. X. Han, "Optical emission in magnetically confined laser-induced breakdown spectroscopy," *Journal of Applied Physics*, vol. 100, no. 5, pp. –, 2006.

[48] L. Guo, W. Hu, B. Zhang, X. He, C. Li, Y. Zhou, Z. Cai, X. Zeng, and Y. Lu, "Enhancement of optical emission from laser-induced plasmas by combined spatial and magnetic confinement," *Opt. Express*, vol. 19, no. 15, pp. 14 067–14 075, Jul 2011.

[49] L. B. Guo, B. Y. Zhang, X. N. He, C. M. Li, Y. S. Zhou, T. Wu, J. B. Park, X. Y. Zeng, and Y. F. Lu, "Optimally enhanced optical emission in laser-induced breakdown spectroscopy by combining spatial confinement and dual-pulse irradiation," *Opt. Express*, vol. 20, no. 2, pp. 1436–1443, Jan 2012.

[50] Z. Hou, Z. Wang, J. Liu, W. Ni, and Z. Li, "Combination of cylindrical confinement and spark discharge for signal improvement using laser induced breakdown spectroscopy," *Opt. Express*, vol. 22, no. 11, pp. 12 909–12 914, Jun 2014.

[51] V. Babushok, F. D. Jr., J. Gottfried, C. Munson, and A. Miziolek, "Double pulse laser ablation and plasma: Laser induced breakdown spectroscopy signal enhancement," *Spectrochimica Acta Part B: Atomic Spectroscopy*, vol. 61, no. 9, pp. 999 – 1014, 2006.

[52] D. N. Stratis, K. L. Eland, and S. M. Angel, "Dual-pulse LIBS using a pre-ablation spark for enhanced ablation and emission," *Appl. Spectrosc.*, vol. 54, no. 9, pp. 1270–1274, Sep 2000.

[53] J. Scaffidi, J. Pender, W. Pearman, S. R. Goode, B. W. Colston, J. C. Carter, and S. M. Angel, "Dual-pulse laser-induced breakdown spectroscopy with combinations of femtosecond and nanosecond laser pulses," *Applied optics*, vol. 42, no. 30, pp. 6099–6106, 2003.

[54] D. K. Killinger, S. D. Allen, R. D. Waterbury, C. Stefano, and E. L. Dottery, "Enhancement of Nd:YAG LIBS emission of a remote target using a simultaneous CO2 laser pulse," *Opt. Express*, vol. 15, no. 20, pp. 12 905–12 915, Oct 2007.

[55] M. Weidman, M. Baudelet, S. Palanco, M. Sigman, P. J. Dagdigian, and M. Richardson, "Nd:YAG-CO2 double-pulse laser induced breakdown spectroscopy of organic films," *Opt. Express*, vol. 18, no. 1, pp. 259–266, Jan 2010.

[56] O. A. Nassef and H. E. Elsayed-Ali, "Spark discharge assisted laser induced breakdown spectroscopy," *Spectrochimica Acta Part B: Atomic Spectroscopy*, vol. 60, no. 12, pp. 1564 – 1572, 2005.

[57] W. Zhou, K. Li, Q. Shen, Q. Chen, and J. Long, "Optical emission enhancement using laser ablation combined with fast pulse discharge," *Opt. Express*, vol. 18, no. 3, pp. 2573–2578, Feb 2010.

[58] L. Liu, S. Li, X. N. He, X. Huang, C. F. Zhang, L. S. Fan, M. X. Wang, Y. S. Zhou, K. Chen, L. Jiang, J. F. Silvain, and Y. F. Lu, "Flame-enhanced laser-induced breakdown spectroscopy," *Opt. Express*, vol. 22, no. 7, pp. 7686–7693, Apr 2014.

[59] L. Liu, X. Huang, S. Li, Y. Lu, K. Chen, L. Jiang, J. Silvain, and Y. Lu, "Laser-induced breakdown spectroscopy enhanced by a micro torch," *Optics Express*, vol. 23, no. 11, pp. 15 047–15 056, 2015.

[60] Y. Liu, M. Baudelet, and M. Richardson, "Elemental analysis by microwave-assisted laser-induced breakdown spectroscopy: Evaluation on ceramics," *J. Anal. At. Spectrom.*, vol. 25, pp. 1316–1323, 2010.

[61] Y. Ikeda and R. Tsuruoka, "Characteristics of microwave plasma induced by lasers and sparks," *Appl. Opt.*, vol. 51, no. 7, pp. B183–B191, Mar 2012.

[62] B. Kearton and Y. Mattley, "Laser-induced breakdown spectroscopy: Sparking new applications," *Nat Photon*, vol. 2, no. 9, pp. 537–540, 09 2008.

[63] Y. Liu, B. Bousquet, M. Baudelet, and M. Richardson, "Improvement of the sensitivity for the measurement of copper concentrations in soil by microwave-assisted laser-induced breakdown spectroscopy," *Spectrochimica Acta Part B: Atomic Spectroscopy*, vol. 73, no. 0, pp. 89 – 92, 2012.

[64] Y. Ikeda and R. Tsuruoka, "Microwave-enhanced emission intensity and plasma lifetime in laser-induced breakdown spectroscopy," *50th AIAA Aerospace Sciences Meeting including the New Horizons Forum and Aerospace Exposition*, 2015/04/28 2012.

[65] A. Khumaeni, T. Motonobu, A. Katsuaki, M. Masabumi, and W. Ikuo, "Enhancement of LIBS emission using antenna-coupled microwave," *Opt. Express*, vol. 21, no. 24, pp. 29 755–29 768, Dec 2013.

[66] M. Tampo, M. Miyabe, K. Akaoka, M. Oba, H. Ohba, Y. Maruyama, and I. Wakaida, "Enhancement of intensity in microwave-assisted laser-induced breakdown spectroscopy for remote analysis of nuclear fuel recycling," *J. Anal. At. Spectrom.*, vol. 29, pp. 886–892, 2014.

[67] R. C. Chinni, D. A. Cremers, L. J. Radziemski, M. Bostian, and C. Navarro-Northrup, "Detection of uranium using laser-induced breakdown spectroscopy," *Appl. Spectrosc.*, vol. 63, no. 11, pp. 1238–1250, Nov 2009.

[68] D. A. Cremers, A. Beddingfield, R. Smithwick, R. C. Cinni, C. R. Jones, B. Beardsley, and L. Karch, "Monitoring uranium, hydrogen, and lithium and their isotopes using a compact laser-induced breakdown spectroscopy (LIBS) probe and high-resolution spectrometer," *Appl. Spectrosc.*, vol. 66, no. 3, pp. 250–261, Mar 2012.